universität wien

MASTERARBEIT | MASTER'S THESIS

Titel | Title

Sonifying Optical properties Using Nanotube Data
A new way of data analysis targeting an auditive interpretation of optical absorption spectra

verfasst von | submitted by

Bernadette Czermak BSc

angestrebter akademischer Grad | in partial fulfilment of the requirements for the degree of

Master of Science (MSc)

Wien | Vienna, 2025

Studienkennzahl lt. Studienblatt | Degree programme code as it appears on the student record sheet:	UA 066 876
Studienrichtung lt. Studienblatt | Degree programme as it appears on the student record sheet:	Masterstudium Physics
Betreut von | Supervisor:	Univ.-Prof. Dr. Paola Ayala

Acknowledgments

This thesis concludes my studies in Physics at the University of Vienna. As such, I want to acknowledge everyone and show my appreciation to the people who contributed to this project, whether directly or indirectly. Your support has been invaluable, and I am truly grateful!
First, I want to express my gratitude towards Univ. Prof. Dr. Paola Ayala for agreeing to supervise this thesis and providing me the opportunity to chase after one of my passions. Without her support, I would not have had the chance to gain experience in sonification, which I value greatly.
To the division for Media and Information Technology at Linköping University, for offering suggestions to this work, which have improved the quality of the text immeasurably. I further want to thank Senior Ass. Prof. Niklas Rönnberg for enabling me to delve deeper into the matter of sonification and always making time for my questions.
I want to extend my gratitude to the Vienna Doctoral School of Physics for their financial support, which allowed me to use my full focus and potential to complete this work. Additionally, I also want to thank the committee of the kwA for granting me the financial support to attend the short scientific residency at the Linköping university in Sweden, which enabled me fruitful insights and the opportunity to form new friendships.
I want to thank all encounters along the way who shaped my way of thinking throughout the years.
To my family and friends, I am eternally grateful for the support and encouragement to follow my ideas.
I want to thank Ruth and Thomas, for the discussions and support of all kind. Thank you for always being there and not only keeping up, but supporting me with my decisions.
Flo, my beloved partner, thank you for not only the mental support but all the inspiring late night discussions. Thank you for supporting my visions and being part of my journey, it is indescribable how much that means to me.

Abstract

Sonification represents a research field in which the audible representation of data, that is usually visualized graphically, is targeted. In short, the translation of data into sounds is studied. This work aims to introduce and explore sonification together with aspects of the solid state physics of carbon nanotubes. The conceptual work towards first sonification concepts of optical absorption spectra of selected nanotube chiralities (9,1), (9,2) and (6,5) is presented and studied. The project targets the first steps towards an auditive distinction of different nanotube chiralities for blind and visually impaired researchers based on measured optical properties induced by energy band transitions. This is investigated using basic concepts of sonification, focusing on parameter mapping strategies. The results lead to first sound renderings of the three different chiralities. The auditive interpretation of these indicate the complexity of applying the sonification design on a large data set. This leads to the conclusion that an additional sonification design is required in the future. However, for the early stages of this project, the most promising concept is provided by an appropriately mapped sonification of the most crucial sections of the spectrum in the wavenumber range between 8500 cm^{-1} and 18500 cm^{-1}. The assessment of the validity and reliability of the approaches is based on personal proofs of concept, which lead to the conclusion that more research needs to be conducted for a complete audible understanding of the physical processes in nanotube data. Therefore, the consideration of additional data dimensions and the use of different kinds of nanotube data that facilitate the distinction of different chiralities are needed. One such concept involves the investigation of the (color) behavior exhibited by soluted single-walled carbon nanotubes. Along with other suggestions, the discussion chapter highlights different arguments for the consideration in further/future development of this project.

Kurzfassung

Sonifikation beschäftigt sich mit einer hörbaren oder auditiven Darstellungsmöglichkeit von Daten, die normalerweise graphisch (visuell) dargestellt werden. Kurzgefasst ist Sonifikation die Übersetzung von Daten in Töne. Diese Arbeit soll in diese Thematik im Zusammenhang mit der Festkörperphysik von Kohlenstoffnanoröhrchen und deren optischen Eigenschaften einführen. Konzepte für erste Sonifikation von halbleitenden einwandigen Kohlenstoffnanoröhrchen der ausgewählten Chiralitäten (9,1), (9,2) und (6,5) und deren optischen Absorptionsspektren werden beleuchtet. Das Ziel des Projekts ist für blinde und sehbehinderte Forscher ein Konzept zur auditiven Interpretation von Kohlenstoffnanoröhrchen-Spektra zu kreieren und damit eine Unterscheidung von verschiedenen Chiralitäten zu ermöglichen. Dafür werden verschiedene Konzepte vorgestellt die vor allem verschiedene Parameter Mappings untersuchen. Die erhaltenen ersten Tonausgaben weisen darauf hin, dass die Analyse mit den in dieser Arbeit erarbeiteten Konzepten zu komplex für große Datensets ist. Daher ist weitere Forschung und Weiterentwicklung dieser sowie anderer Konzepte notwendig. Für das frühe Stadium dieses Projekts zeigen zwei Konzepte einen vielversprechenden Startpunkt für vertiefendere Forschung. Diese sind das Konzept der Sonifikation von essenziellen Abschnitten der Spektren im Wellenzahl-Bereich von 8500 cm^{-1} und 18500 cm^{-1} mit Hilfe eines passenden "mappings" in Kombination mit sogenannten "Earcons". Die Prüfung der verschiedenen Konzepte auf Gültigkeit und Zuverlässigkeit basiert auf ”proofs of concept” deren Interpretation auf einer persönlichen Auswertung basieren. Daraus lässt sich schließen, dass für eine komplette Analyse der Daten und Eigenschaften von einwandigen Kohlenstoffröhrchen in einem nächsten Schritt mehr Datendimensionen der Spektren in die Sonifikation miteingebunden werden müssen. Darüber hinaus soll ein weiteres Konzept, das sich mit der Farbabhängigkeit verschiedener Chiralitäten beschäftigt, ein komplimentäres Bild schaffen. Zusammen mit anderen Vorschlägen, bietet das Diskussions- und Abschlusskapitel dieser Arbeit Einblicke in zukünftige und vertiefende Möglichkeiten für die Weiterentwicklung dieses Projekts.

Contents

1 Introduction

According to the World Health Organization (WHO), about 2.2 billion people worldwide live with some kind of vision impairment, which accounts for roughly a fourth of the global population [1]. Around 43 million of those are blind and almost 300 million have a strong visual impairment [2].

Hence, the steady demand for improvements in accessibility for the Blind/Visually Impaired (B/VI) plays an important role also in terms of Data Analysis, which will also benefit people with dyslexic disabilities.

Sonification in simple terms can be understood as the translation of data into sounds, which forms a research field with growing interest and attention not only towards applications for the B/VI but also in the field of science communication and public outreach [3]. Additionally, sonification opens up a new world with different means of interpreting data and provides the potential to allow faster data analysis [4]. Different projects targeting the translation of data into sounds have been attempted before in various fields [5]. Some examples can be found in the field of Astrophysics and Astronomy, e.g. "Sonification from NASA telescopes" [6]. Projects in Environmental Science include "Songs of the Tides" [7], and others like "A Symphony of Bureaucracy" [8].

The rising interest in understanding single-walled carbon nanotubes (SWCNT) and their outstanding properties lays the foundation for this work. Pairing this topic with sonification represents a new and fascinating research direction worth exploring. Due to the (almost) one-dimensionality of SWCNTs through their high aspect ratio, unique optical and electronic properties are revealed, introducing van Hove singularities into the density of states [9]. The main characteristics of SWCNTs are described by their chirality and electronic structure, hence the determination of these parameters is of utmost importance for basic research [10]. Raman spectroscopy, Photoluminescence spectroscopy (PLS), and Optical Absorption spectroscopy (OAS) provide techniques with which optical and electronic properties can be uncovered, a crucial step in the development of new applications and ongoing research [9]. OAS represents a fundamental way of probing SWCNT samples, proving to be a non-destructive method and providing output in form of transmission or absorption spectra. To be able to draw conclusions about the optical properties of an individual SWCNT, its chirality has to be determined first. With the usage of PLS the chirality of SWCNTs can be revealed, enabling the comprehensive interpretation of optical absorption spectra [10]. As the properties of SWCNTs are still not fully understood, the demand for investigating these spectra is highlighted. Enabling B/VI researchers the opportunity to analyze them within a new approach will provide the field with more opportunities to comprehend the behavior of SWCNTs differently and possibly faster, in addition to enabling a larger group of people to work in this field.

The aim of this thesis is to explore sonification of OAS for revealing optical properties

of SWCNT auditively. The application of sonification to SWCNT data has not been attempted or explored before. To tackle the problem statement, the work has aimed to answer the following research questions:

- Which optical properties can be considered for the translation?
- In which way can these optical properties be put into sounds?
- What represents an appropriate parameter mapping for the optical properties that are aimed to be sonified?

As the contents of this thesis will elaborate, the answers to these questions are not trivial. However, the thesis is structured in a way that will lead towards an understanding of these questions.

Throughout the thesis, the fundamentals of the physics behind SWCNTs are provided in addition to a framework for a theoretical understanding of sonification which will be elaborated. The goal of the thesis is not only to present an appropriate data translation in form of parameter mapping, but to connect the two fields and pave the way from the theoretical basis to the translation of OAS into a sonified output and with that laying the foundation for a later tool development.

Chapter 2 of the thesis will reflect on and connect the theories of optical properties of SWCNTs and sonification. In the first part of Material and Methods (chapter 3), the experimental data collection is explained, while the second part focuses on the different concepts used for the translation of the data. After the presentation of the Results (chapter 4) and their Discussion (chapter 5), recommendations for future research projects will be given in the final chapter.

2 Background

In order to find and understand the answers to the research questions posed in the previous section, an excursion into solid state physics is necessary. Moreover, it is necessary to take a leap towards the theory of auditory display with a special focus on sonification.

2.1 Semiconductors

Research on semiconductors was first conducted in the 19^{th} century when the investigation of electronic properties of materials began [11]. Seebeck, who is today widely known for the Seebeck-effect which relates the conversion of temperature and electric voltage through thermo-coupling, contributed to the discovery of semiconductors through his research. He noticed an amplification of the Seebeck effect when applied to semiconductors [12]. This discovery was made in 1821, and was a stepping stone for further exploration of different materials that opened various new fields. In the beginning of the 20^{th} century, the collected results up until this point led to the conclusion that for the description of the various phenomena occurring in different materials, a comprehensive theory of solid state physics was required, which was later got expanded using insights from the theory of quantum mechanics [12]. Around 1914 the classification of metals, insulators and "variable conductors", which later received the name semiconductors, was established [13]. Around the 1950's the invention of the transistor led to a boom in the semiconductor industry that has lasted until today [11].

Nowadays semiconductors are classified based on their electrical resistivity or their energy band gap determined by the band structure of a material (valence band (VB) and conduction band (CB) for semiconductors) [14]. Semiconductors appear in a large variety of crystal structures and can be either from metallic elemental origin (Si), based on binary compounds (GaAs) or from organic origin (C and SWCNTs) [14].

2.2 Carbon Nanotubes

Carbon is a versatile element exhibiting various properties in different configurations and bonding states, leading to various materials, components and applications that are of big interest in multiple branches of research [15]. These include the research and development of solar cells, biomedical applications, and electronic components to name a few [9]. The exact time of the discovery of carbon nanotubes (CNTs) is still under discussion [11], however some sources estimate the discovery to have occurred around the mid 20^{th} century [16], about the same time as the invention of the transistor. CNTs represent an allotrope of carbon, with unique conductive properties, which play an important role in the field of

material science. The structure of a CNT can be described with a monoatomic layer (or sheet) of graphene, which is rolled up into a tubular shape. There is a distinction between single-walled (SWCNTs) and multi-walled CNTs (MWCNTs), the former consisting out of one layer of graphene and the latter out of multiple sheets, respectively.

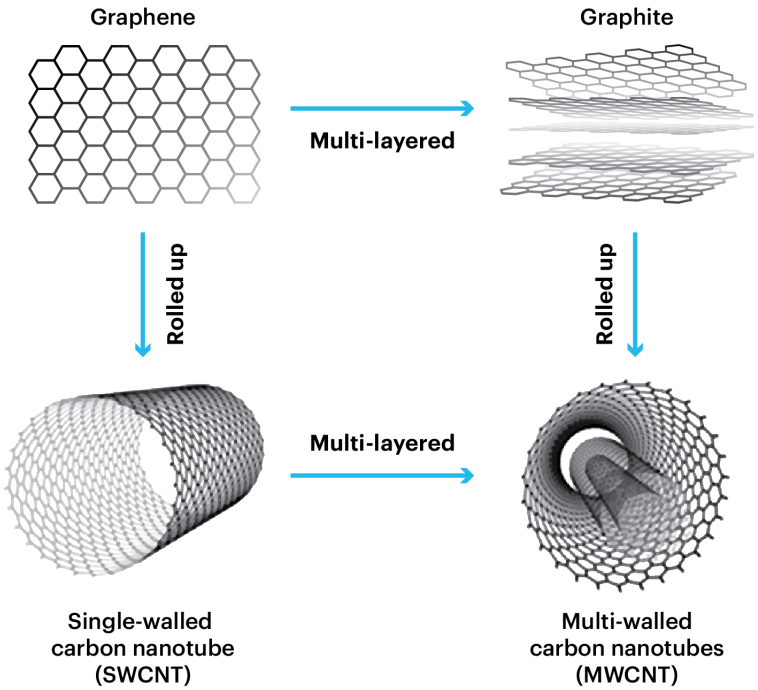

Figure 2.1: Structure of graphene (top left) and SWCNT (bottom left) as well as MWCNT (bottom right), graphic taken from [17].

Graphene (as well as Graphite) is referred to as conjugated system, meaning the system consists out of π-conjugations (connected p-orbitals) with delocalized electrons in the molecule, which lower the overall energy of the molecule and increases its structural stability [15]. Figure 2.1 depicts the correlation between different CNTs. The exploration and understanding of CNTs and their properties will allow the further development of novel materials and new technological applications. As CNTs show peculiar optical behavior, the motivation to explore these properties is evident [18].

In general, CNTs have a strong tendency to form bundles due to van der Waals interactions, causing electronic coupling in between the bundles, which imposes the challenge of obtaining pure chirality sorted SWCNT samples. The properties of CNTs are strongly governed by the structure and defects of the graphene lattice. Any modulations of the lattice through defects, doping or chemical functionalization will strongly influence the properties of the CNT accordingly [14]. There is a distinction between structural properties, including circumference, length and numbers of walls, electronic properties, referring to the bonding between the carbon atoms, as well as chirality and optical properties, which describe the interaction between light and matter (SWCNTs) [9].

2.2.1 Structural and Electronic Properties

The individual carbon atoms of a CNT are bonded through covalent bonding and therefore exhibit $sp^{2+\delta}$ hybridization [9]. This implies a variation between sp^2 and sp^3 and therefore can be classified as a structure between Graphene and Graphite. Further, Graphene as well as Graphite mainly consist out of π-conjugations, which are apparent in the density of states (DOS) [9]. The magnitude of the circumference of CNTs usually lies around $d = 1$ nm and the respective length varies from nanometers to millimeters. This reveals the crucial property, the high aspect ratio, which enables the characterization of CNTs as nanostructured (almost) one-dimensional materials [15]. Another important structural property, which simultaneously reveals electronic properties, is introduced by the chirality or chiral angle expressed as

$$c = (n, m). \tag{2.1}$$

Conceptually and hence mathematically, the chirality is determined by the angle in which the graphene layer is rolled up [9]. Its description is derived using the (mathematical) descriptions of real and reciprocal space. Figure 2.2 represents a graphene lattice with all parameters necessary to construct the chiral vector. These include the chiral angle θ and the chiral vector defined as $\vec{C} = n\vec{a}_1 + m\vec{a}_2$, where n and m are integers and $\vec{a}_1$ and $\vec{a}_2$ lattice basis vectors.

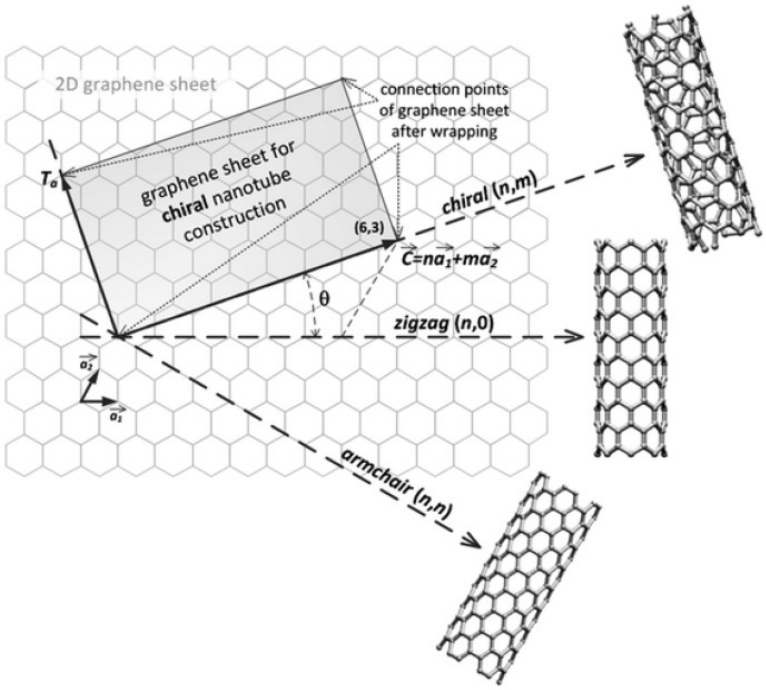

Figure 2.2: Graphical representation of the chiral angle when rolling up a graphene sheet. Graphic taken from [19].

The individual chirality or angle used to roll up the nanotube results in an individual

structure of the nanotube, which can also be classified using the description of armchair, chiral, or zigzag nanotube, visually represented in Figure 2.3. SWCNTs can be separated

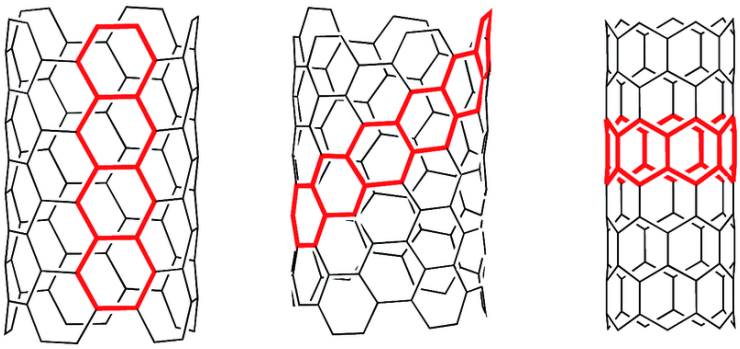

Figure 2.3: Visual representation of armchair (left), chiral (middle) and zigzag (right) nanotube. Graph adapted from [20].

and sorted according to their chirality, posing not a trivial task [21], which is why researchers are investigating techniques to determine the best technique (ranging from synthesis and nanotube growth and characterization.) [22]. The importance of working with (purely) chirality sorted SWCNT samples is emphasized depending on the application or project. This thesis and its concepts, in particular, makes use of chirality sorted samples (Chapter 3 SWCNT samples).

The nanostructure of the SWCNT, including alignment along with the structural properties, such as size, defects, bonding, etc. exhibits remarkable electronic properties [10]. Examples for these are electrical conductivity and dielectric response. Knowledge of (n, m), along with the information about size and defects in the lattice, allows the characterization of different SWCNTs based on their conductivity. The two most commonly occurring types are metallic or semiconducting SWCNTs [9], [18]. Table 2.1 represents the classification according to the chirality of individual SWCNT and lists their average band gap energy. The distinction between different chiralities shows that all armchair SWCNTs are metals.

description	**(n, m)**	**conductivity**
armchair	$n = m$	metallic
zigzag	$m = 0$	semiconducting
chiral	$n \neq m$	semiconducting

Table 2.1: Classification of different CNT's according to their conductivity and chirality.

Those for which

$$n - m = 3j, \tag{2.2}$$

where $(j \neq 0)$, are semi-metals since tube curvature effects create a small band gap [23]. The remaining two types of SWCNTs, zigzag and chiral, are semiconductors with band gaps inversely proportional to their diameters.

In the frame of this thesis only semiconducting SWCNTs and their properties are considered.

2.2.2 Optical Properties of Semiconducting SWCNTs

Optical properties are investigated by their absorption, Photoluminescence (PL) and Raman spectra [9]. The use of the respective spectroscopy techniques reveals the structure and excitonic nature of the SWCNT, enabling the description of its excitation states [9]. Optical properties are also described by optical physics, including the consideration of phenomena such as reflection and transmission, scattering, in addition to absorption and luminescence. These properties strongly depend on chirality as each type of SWCNT has a unique set of absorption peaks which correlate with the van Hove singularities in the DOS [23]. Different mechanisms appear during the interaction with light. When considering the absorption process for example, the absorption of photons can lead to conduction in a semiconducting SWCNT, due to the band-to-band transitions. After a characteristic time the electrons relax back into a lower energy state, which can lead to the emission of photons. Due to this interaction with light, SWCNTs exhibit different colors in solution (Figure 2.4). Based on available SWCNT data, a quantitative model

Figure 2.4: Colours of metallic and semiconducting SWCNTs with different diameters, graphic taken from [9].

can be formulated to describe the relation between color and chirality, which appears to be diameter dependent. With this model, the coloration mechanisms of hundreds of chiralities can be determined [24]. This highlights the variety of properties SWCNTs display and can act as a complimentary description to their microscopic properties.

2.3 Optical Absorption

Optical Absorption denotes the process of an incoming photon being absorbed by a quantum system, also referred to as an electric dipole interaction. Considering a semiconducting SWCNT, the resulting energy gain leads to a promotion of an electron from the VB into the CB, from lower to higher energy state, respectively [25]. The (theoretical) positively charged hole which is left behind in the VB forms an exciton together with the negatively charged electron due to the Coulomb interaction between charges. The light matter interaction processes in SWCNTs can be described by this quasi-particle [9].

Considering a classical semiconductor, like GaAs for example, different band-to-band transitions can occur, depending on the energy of the interacting photons [26]. There are four typical transitions that can appear: At very low energies (below 0.1 eV) phonon absorption occurs. This is caused by the energy released from the scattering of the absorbed photons which creates vibrations in the lattice (phonons). Intraband transitions describe the transitions within a band which usually occur below the band gap energy, which is between 0.1 eV and 1 eV in this example (Figure 2.5).

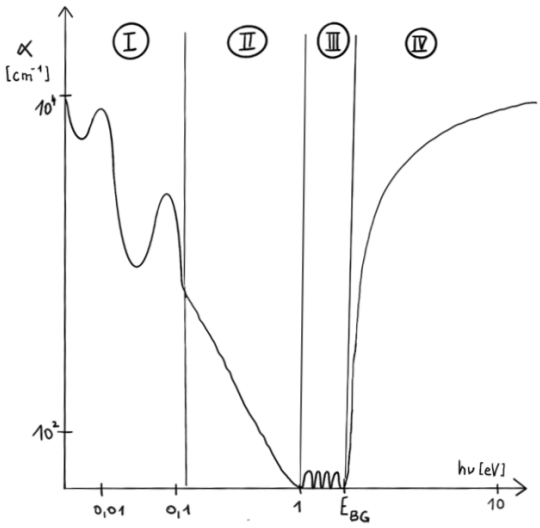

Figure 2.5: Exemplary absorbance of a classical semiconductor (GaAs) and its different transitions divided into 4 different regions, graphic adapted from [26]. I: Phonon absorption; II: Intraband transitions (free carrier absorption); III: Excitonic vibrations; IV: Interband transitions;

Just below the band gap energy, the excitonic resonances appear, which refer to e^{-}-h pairs being excited. Interband transitions describe the band-to-band transitions from the VB to the CB. These typically occur in the energy range of the material's band gap energy and beyond [26]. As the energy transitions and hence the peaks in the OA spectra in a semiconducting SWCNT are visible beyond the band gap energy, only Interband transitions are considered.

The absorption of photons induces a series of different processes, including different band-to-band transitions, leading to different optical properties which can be investigated by OAS, PL, and Raman spectroscopy. However, before understanding the band-to-band transitions, the introduction of van Hove singularities into the density of states need to be understood along with the theoretical aspects of phonons and their dispersion relation.

2.3.1 Density of States and Energy Transitions

The density of states (DOS) is used to describe the allowed electronic states per unit energy [14]. In contrast, the joint density of states (JDOS) reveals the allowed energy transitions fromVB to CB [27]. The latter is used to describe optical processes. The 2D and 3D representation in the JDOS can be seen in figure 2.6. Due to the small dimensions

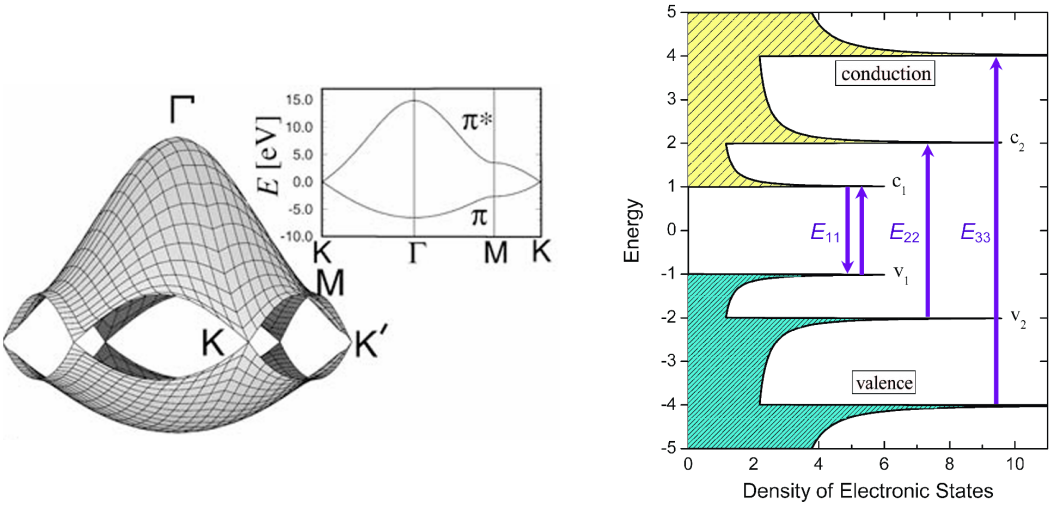

Figure 2.6: Left: Band structure of a SWCNT [18]. Right: Band structure in the density of states showing the energy transitions between the first three bands [28].

of CNTs which lie in the same range as the wavelength of light, the optical behavior of SWCNTs exhibits a molecular nature as well as a solid state nature [25]. The former refers to the quantization of k-vectors along the circumferential direction, which gives rise to sharp van Hove singularities in the JDOS. The CB and VB, which consist of π-electron states, touch at the corners of the hexagonal Brillouin zone (BZ), known as the K and K' points, where E_{ii} becomes singular. These non-differentiable points are referred to as van Hove singularities [9].

Within the solid state nature, k is continuous in the direction of the nanotube axis and scattering or relaxation behavior occurs by phonons or conduction electrons. These factors give rise to the unique behavior in the optical properties [10]. The right hand side of figure 2.6 shows the energy in dependence of the density of electronic states. The band-to-band transitions appear from the first VB to first CB as well as between the other bands, respectively [10].

The absorption of one or multiple photons by a semiconducting SWCNT initiates a series of processes that lead to different optical properties [9]. The theory of nanostructured materials in solid state physics helps to describe and understand the occurring processes qualitatively. If the energy of the incident photon is higher than the energy of the band gap (E_{BG}) of the semiconducting SWCNT, an electron can transition into the CB through absorption. In other words, the absorption in a SWCNT relates to their

electronic transitions E_{ii}, which manifest as sharp peaks in measured spectra. These can be used to identify SWCNT types, since every chirality features characteristic peaks in the absorption spectra. However, these peaks tend to either overlap or look similar for different chiralities. Therefore, to enable a full description and precise distinction of the individual SWCNTs, Photoluminescence (PL) maps and Raman spectroscopy are used.

2.3.2 Phonons and their Dispersion Relation

The phonon dispersion relation is another important characteristic of a SWCNT, hence a short excursion into its theory should provide an additional concept with which the properties of SWCNTs can be explained and Raman spectra understood [18]. Phonons in solid state physics are vibrations between interacting particles in a lattice [29]. They are also referred to as quantized sound waves, which can exhibit acoustic and optical phonons, which distinction based on how the phonons propagate in a solid [30]. For long wavelengths the propagation of acoustic phonons can lead to sound, as for those cases the dispersion relation is almost linear, which leads to the interpretation that phonons with small k can propagate over long distances within a lattice (leading to a sound).

Phonons can be excited through photons and show characteristic behavior depending on which kind of phonon is being excited. Figure 2.7 graphically represents the different modes within the first BZ.

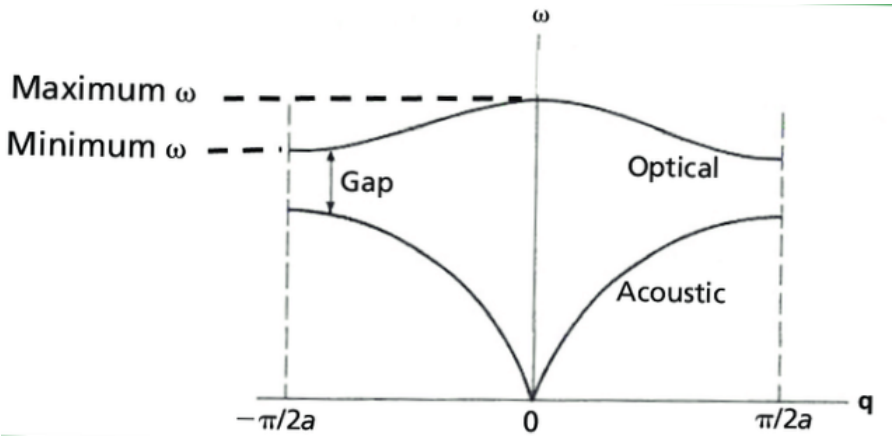

Figure 2.7: Phonon dispersion curve for a linear diatomic lattice in the first BZ, adapted from [31].

Considering a $3D$ solid, $3N$ represents the number of possible phonons (N represents the number of atoms in the solid). Based on that the occurrence of phonons is divided into 3 acoustic phonons and $3N - 3$ optical phonons.

The speed of the propagation of (acoustic) phonons can be determined by the first derivative of the dispersion relation [18]:

$$v_{group} = \frac{\delta\omega}{\delta k}, \tag{2.3}$$

where the dispersion relation is the correlation of frequency and wavenumber

$$\omega = \omega(k), \tag{2.4}$$

revealing information about the DOS or the corresponding van Hove singularities for SWCNTs [18]. Its understanding can be approached in different ways. The two most prominent approaches for the calculation of the phonon dispersion relation include (i) zone folding (ZF) of phonon dispersion curves for a single 2D graphene sheet and (ii) through ab-initio calculations [32].

In approach (i) the 1D phonon dispersion relation can be expressed through the 2D graphene phonon dispersion relation [33]:

$$\omega_{\mathrm{1D}}^{m\mu}(k) = \omega_{\mathrm{2D}}^{m}(k\frac{K_2}{|K_2|} + \mu K_1). \tag{2.5}$$

Here, K_1 and K_2 are the reciprocal lattice vector along the nanotube axis and in the circumferential direction. Through this ZF approach the radial breathing mode RBM of a Raman spectrum, which is explained below, can be determined along with the diameter of the nanotube, which highlights the importance of this concept.

2.3.3 Raman Spectroscopy

A solid material can be characterized by their individual phonon modes. Raman spectroscopy targets the exploration of the vibrational modes of molecules [18], which complements the information about the electronic structure and optical properties of CNTs, respectively. This technique investigates the inelastic light scattering between photons and optical phonons, which are described by Raman scattering. This can either lead to Stokes Raman scattering or Anti-Stokes Raman scattering (Figure 2.8).

The incident photons interact with molecular vibrations and phonons. As a result, the interactions lead to promotion or relaxation between the bands. The energy difference between the incoming and outgoing photon is referred to as the Raman shift. When the energy of a Raman active phonon of two different samples are known, the sample can be identified using Raman spectroscopy [35]. Graphene shows two peaks, one appearing around $1580cm^1$, called the G band, and the other peak appears around $2700cm^1$, which is called the G' band [35]. They are associated with vibration of carbon atoms [18]. Peaks that are located in low wavenumbers are generally associated with interactions at the circumference of the nanotube. A unique vibration in graphene-like materials like SWCNTs for example, is called the radial breathing mode (RBM). It can describe the carbon nanotube content in a sample [36]. In addition, acoustic modes give rise to the RBM and together with the knowledge about the frequency of the occuring RBM, the diameter of the nanotube can be estimated [18].

2.3.4 Optical Selection Rules

The description of possible optical transitions can be expressed through the formalism of electromagnetism, stating whether a given transition is allowed or not. For the mathematical description, the direction of the applied field polarization of light is considered [25].

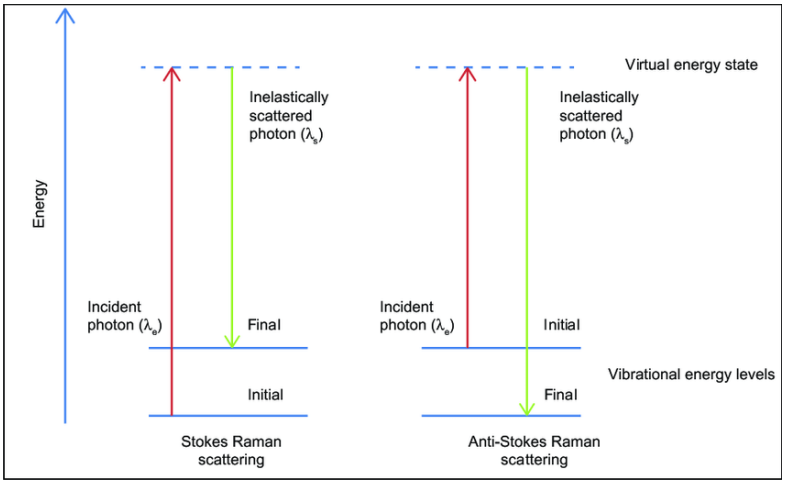

Figure 2.8: Schematic showing the difference between Stokes and anti-Stokes Raman scattering. Graphic taken from [34].

When light interacts with graphite, it is strongly absorbed when incident perpendicular to the graphite plane. The electrical field changes sinusoidally on the cylindrical (SWCNT) surface when entering perpendicular, allowing the optical transitions from band indices differing by ± 1 from each other [25].

At parallel polarization, the external field on the nanotube surface is constant, therefore allowing optical dipole transitions to manifest [25]. Due to the 1D lattice structure of SWCNTs, the optical absorption for light polarized parallel to the nanotube axis is strongly enhanced and the absorption for perpendicularly polarized light is strongly suppressed in both an aligned SWCNT bundle, or an isolated SWCNT. This effect is also known as the depolarization effect [10]. The selection rules depending on the polarization of the light can be formulated accordingly. Whenever the light is parallel polarized, optical transitions are allowed between bands with same band index. Moreover, optical transition are forbidden for metallic SWCNTs between linear CBs and VBs [25]. For perpendicular polarized light, optical transitions are allowed between bands whose band indices differ by ± 1. Transitions between band-edge states having the same eigenvalues are allowed, while those with different eigenvalues are forbidden [25].

2.3.5 Optical Absorption Spectroscopy (OAS)

OAS provides useful information on the composition and distribution of individual SWCNTs dispersed in solution. As MWCNTs have less-defined absorption features due to wall-to-wall electronic coupling and spectral overlapping in a heterogeneous mixture, SWCNTs represent the optimal probing material for OAS results that can be used as a theoretical basis.

The aim of the measurement of OAS is to determine how much light is absorbed by a sample at each measured wavelength. To be able to measure several wavelengths at

constant resolution simultaneously, Fourier Transform Infrared Spectroscopy (FTIS) is used. The speed and sensitivity afforded by FTIS is another advantage of the technique [37]. In this method, the probing beam is generated by an IR irradiation source that emits polychromatic light. After passing through a Michelson Interferometer, the outgoing beam is directed through the sample. Due to light wave interference, different wavelengths are modulated at different rates, so that at each moment or mirror position the beam coming out of the interferometer shows a different spectrum [37].

This can be explained using the mathematical description of the Fourier transform: The function f transforms a function g which depends on variable δ into another function h depending on ν (where g and h are known as Fourier pairs). The basic form of the Fourier transform can be expressed by

$$f(x) = \frac{A_0}{2} + \sum_{n=1}^{\infty}(A_n \cos\left(\frac{n\pi x}{c}\right) + B_n \sin\left(\frac{n\pi x}{c}\right)), \tag{2.6}$$

where A_0 can be expressed by

$$\frac{A_0}{2} = \frac{1}{2c}\int_{-c}^{c} f(x)dx. \tag{2.7}$$

FTIS is a technique using an optical component to produce $g(\delta)$ over a range of δ values [37]:

$$h(\nu) = \int_{-\infty}^{\infty} g(\delta)e^{i2\pi\nu\delta}d\delta, \tag{2.8}$$

$$g(\delta) = \int_{-\infty}^{\infty} h(\nu)e^{-i2\pi\nu\delta}d\nu, \tag{2.9}$$

where the range of values of the variable δ, which is used to determine $g(\delta)$ during a measurement, will be limited to an interval smaller than $(-\infty, \infty)$ [37]. The signal that is retrieved is an interferogram showing characteristics depending on the measured sample, used beam-splitter and irradiation source. The spectrum $S(\nu)$ is revealed with

$$S(\nu) = C\int_{-\infty}^{\infty}[\tilde{I}(\delta) - \frac{1}{2}\tilde{I}(0)]e^{-i2\pi\nu\delta}d\delta, \tag{2.10}$$

with the intensity relating to the Fourier integral. The intensity represents the optical path difference, where $\tilde{I}(0)$ is the signal intensity at $\delta = 0$. The spectrum contains a certain degree of lost information caused by the optical path. The relation with which these losses can be described by contains the resolution $\Delta\nu$ and mirror displacement δ in the expression

$$\Delta\nu = \frac{1}{\delta} = \frac{1}{2L}. \tag{2.11}$$

With the measurement of OAS the determination of several material properties is possible [38]. The intensity graph reveals not only information about the strength of the photon-matter interaction (strong absorption means strong interaction and vice versa),

but also enables interpretation of specific optical properties as well as estimates Coulomb-interaction strength of excitons [25]. Further, the band gap energy can be analyzed. There is a correlation between wavenumber and band gap energy that suggests the higher the value of the wavenumber, the more energy is required for absorption and hence excitations to appear. The following equation represents the correlation between Energy, wavelength and wavenumber:

$$E = h \cdot f = h \cdot \frac{c}{\lambda} = h \cdot c \cdot \tilde{\nu}. \tag{2.12}$$

The peaks in the spectrum refer to the different band-to-band transitions and are expected in certain ranges (see Table 2.2) [39], [40].

Transition	$\lambda[nm]$	range
E_{11}	800-1400	NIR
E_{22}	400-800	VIS
E_{33}	100-400	UV

Table 2.2: Typical ranges from energy transitions for small diameter SWCNTs. Here, λ expresses the wavelength of light in nanometers, NIR stands for the range of near infrared light, VIS for the visible range and UV for the ultraviolett range of light, respectively.

2.3.6 Interpretation of OAS and Optical Properties

Optical spectra are simply understood in terms of band-to-band transitions, which explains the relationship between transition energies and structure of SWCNTs. In addition, this picture explains the strong anisotropy of the absorption intensity observed with respect to the polarization of light [25]. The spectrum is most intense when the photon energy matches the energy difference between corresponding van Hove singularities. For semiconducting SWCNTs the first two energy transitions are expected to appear in the NIR and visible parts of the electromagnetic spectrum [40]. Once the absorbed energy dissipates and gets emitted, the system gives rise to photoluminescence.

The chiral indices of individual semiconducting nanotubes are assigned by analyzing their absorption spectra around their first and second optical resonances (E_{11} and E_{22}, respectively). The values of E_{ii} vary depending on the chirality for which a list of predicted values for the respective energy transition can be compared to reference [41]. Semiconducting SWCNTs exhibit sidebands near the first optical resonance, which can also be observed in the measurements done for this thesis. In other words, light absorption at E_{22} is followed by fluorescence emission near E_{11}. The re-emission of photons leads to different colors of the individual SWCNTs diluted in solution. Theoretical descriptions exist that predict the coloration mechanism for SWCNTs [24]. Techniques to provide complimentary information about the nanotube structure and properties in addition to OAS are Photoluminescence and Raman spectroscopy.

2.3.7 Photoluminescence Spectroscopy (PLS)

PLS is used to characterize the optical and electronic properties of semiconducting SWCNTs, by revealing its 1D excitonic nature through the exploration of the excitation states of SWCNTs [42]. The excitation of electrons into a higher state, induced by the absorption of photons, leads to scattering and phonon interactions. Thereby, the electron can relax and fall back into the initial lower energy state. The excitons are recombined and emission of a photon occurs, which is known as photoluminescence [42]. The time differences over which the emissions occur characterize the dominant kind of light scattering phenomena. Luminescence or phosphorescence appear usually in the time range between femtoseconds and milliseconds.

2.4 Sonification

Sonification, or auditory display, is a scientific field examining how the human auditory system can be used as a primary channel for communicating and transmitting information [3]. The research targets all aspects crucial to consider for a human-computer interaction (HCI), such as hardware, software, and modes of interaction to name but a few. Sonification, which presents a core component of an auditory display, is the process of translating data into sounds [43]. Parameter Mapping sonification is the most commonly used sonification approach, and mainly involves the creation of a translation concept with special focus on the data mapping, as well as the choice of sounds and user requirements [4]. Sonification is a complex matter and therefore there exist no single coherent theory of the field which would explain all different types. However, the following examples will guide readers to an understanding of which applications are based on sonification. Further, the distinction of different sonification types, which are explored later in this thesis, is elaborated.

2.4.1 Types of Sonification

Sonification is the first step towards a multi-sensory experience where the design choices depend on the desired function and target group. Sonification together with the use of other media (visual, haptic, ..) will generally improve the understanding of the displayed data [4]. Depending on the designers choice, the representation can be for "ears only" or can consider the use of a "multi-modal display" [3].

The classification into various types or techniques of sonification can be done using different categories. One distinction can be made by comparing event-based and model-based sonification [3]. The former includes the mapping of data parameters to sound parameters. The latter approach is based on a display, which is built through a virtual model whose sonic responses to user input are derived from data. Consequently, in that case the sonification emerges from the reaction of the data-driven model to the actions of the user.

The distinction of the main concepts in sonification is made using the types of (i) audification, (ii) auditory icons, (iii) earcons, (iv) parameter mapping sonification, (v)

model-based sonification. Within the framework of this thesis types (iii) and (iv) are explored.

Type (i) represents the oldest type among all, and targets an isomorphic representation of the data, which in other words is the auditive representation of the identical shape of the data curve. Audification is most commonly applied to get the most direct and simple representation of data from sound. In most cases it will be used for taking a sound and breaking it down in a way that we can visually understand it and construct more data from it. However, this type requires proper data sets which are neither too small nor too large and possess a suitable order criterion and preferably have periodic components. Audification requires that the waveforms be frequency- or time-shifted into the range of audible frequencies for humans, which lie in the range between 20 and 20,000 Hz. [3]

Type (ii), the Auditory Icons, are embedded in our daily lifes. These include the sound that appears when emptying the trash folder on a laptop or the sound of an error window popping up. This type is used to communicate a message as a brief sound, which is used to represent a specific event or action, which mirrors the action in the real world. This is achieved by the systematic variation of simple sonic "atoms". This approach is not well suited for continuous large data streams and takes advantage of the users prior knowledge and natural auditory associations between sounds and their results. In a way, auditory icons are meant to be the auditory equivalent of visual icons and their sounds are an interpretation of an already existing natural sound [4].

The idea of type (iii) is similar to an auditory icon (type (ii)), with the difference that the created sound is not of a natural origin, but is instead an abstract sound. The application of these acoustic symbols are not well suited for continuous large data streams.

Parameter Mapping Sonification, type (iv), represents a sonification which can handle large data streams and is one of the most commonly used types and therefore often referred to when considering sonification. It involves the mapping of data attribute values, or in other words an association of information with auditory parameters. This sonification type uses changes in acoustic dimensions to refer to changes in data dimensions. [3]

Finally, Model-Based Sonification (type (v)) targets a more interactive sonification design especially compared to parameter mapping sonification. In this approach, the data is turned into dynamic models (or processes) rather than directly into sound. Consequently an interaction by the user is required to explore not only the sonification but also the data. [3]

2.4.2 Functions of Sonification

Sonification designs find different applications and functions in the daily life, some more specific and intuitive than others. A sonification can aim to function as an alarm or warning, as in the case of sirens. It can also assist in monitoring processes by representing the status or progress of a workflow. The purpose of sonification can also target data exploration in various forms. It can try to encode or convey information about an entire data set or its relevant aspects, leading to some form of auditive data interpretation [3]. In addition, the function of sonification can also aim at the use in art, entertainment or sports. The function of the sonification in this thesis is the use as as means of data

interpretation. However, before elaborating the developed approaches, different examples of sonification will give an impression of how it is used in different fields.

2.4.3 Examples of Sonification

A clock releasing a ticking noise every second represents an auditory cue for time passing. Another popular invention using sonification is the Geiger-Müller counter [3]. The working principle relies on charged particles that enter a chamber filled with gas. As a reaction, the particles ionize the gas, so that a current can be measured which allows the detection of the particle and produces an audible click per detected particle [44].

Different publications introduce the idea of sonifying colors either in artwork, images or scientific data [45, 46, 47]. One tool converts color information, such as hue, saturation and value attributes, from images or video frames into sound. The information about the different attributes of the image are mapped accordingly to pitch, timbre and loudness [46]. Another publication introduced an interactive musical periodic table that targets the sonification of light frequencies emitted from individual molecules and elements. Therefore, sine waves are generated for each distinct color. For the sounds, the light frequencies are scaled into the audible range resulting in a linear scaling between color and sound [47].

More recent research also linked to the topic of this thesis is the sonification of spectroscopy data. One project deals with the sonification of infrared (IR) spectra using open source programs, where the time is considered as the spectral frequency indicator (x-axis) and pitch correlates to the intensity of the corresponding band absorptions [48]. Another project aims to sonify IR spectra to be able to distinguish different molecules within an acquired spectrum. In that approach, the wavenumber is converted into frequency which is then scaled into the audible frequency range. Specific sounds are assigned to sections of the spectrum which correlate to individual molecules, enabling distinction between different species [49]. A project tied to that idea is dealing with the acoustic conversion of molecular vibrational spectra, which specifically targets the sonification of IR and Raman spectra [50]. The approach exploits that every molecule has an individual spectrum using elementary waveforms, which each depict the temporal variation in data, mapped on different musical parameters such as timbre, pitch, et ecetera. The purpose of that project is to provide an auditive "fingerprint" of the individual molecules to either help with experimental data analysis and pattern recognition or to create sounds for musical composition. These publications, along with a master's thesis dealing with the sonification of spectroscopy data using the programming environment *MAX* [51] provide the basis and inspiration for the concepts developed in this thesis.

When researching already existing work on sonification in regards to SWCNTs, nothing was found. However, some work dealing with CNT membranes for loudspeakers and microphones exist, representing an entirely different branch of research [52, 53]. As the above mentioned projects display, the sonification of spectroscopy data has been attempted already. However, the approach of sonifying optical absorption spectra revealing optical properties of SWCNTs has not been attempted before. Therefore, this thesis aims for a comprehensive explanation of how a sonification design for analyzing CNT data can be developed. Additionally, this thesis acts as guide to be able to understand the sounds

produced as well as to interpret them.

2.4.4 Sound Synthesis and SuperCollider

When considering sonification as a medium for auditive data visualization, another important factor to consider is the sound synthesis, from which the sounds for the sonification can be made. A synthesized sound can be described by a periodic oscillation of waves [54]. Each of these oscillations can be deconstructed by means of Fourier decomposition as a sum of mutually orthogonal basis waves, such as sine waves with different frequency values. The process of adding up such waves to synthesize a sound is called additive synthesis. In addition, noise and overtones may be added to an additive signal, and the compartment waves may also be square, triangle or sawtooth waves. All of these types of waves can of course be decomposed into sine tones as well. Another approach to sound synthesis is the subtractive method where filters and gates are applied to a harmonically rich signal to remove certain frequencies for example. These two paradigms are the main techniques for sound synthesis. However, sound can be further altered through frequency or amplitude modulation.

These methods can be applied in *SuperCollider*, a programming environment for real-time sound synthesis and algorithmic composition [55]. Due to the complexity in operating and coding with *SuperCollider*, it is only introduced with simple coding examples in chapter 3 and the concepts for the sonification of the optical absorption spectra is done in *Python*. However, the importance of considering *SuperCollider* for future implementations of this project are highlighted.

3 Material and Methods

To tackle the research questions posed in chapter 1 and obtain a sonification of SWCNT spectroscopy data, two main tasks need consideration. These include the collection of the OAS data and the signal processing of the data for the sonification design. For the first part, experimental measurements of different SWCNT chirality samples were measured. The signal processing and the sonification were implemented using *Python*.

3.1 Fourier Transform Infrared Spectroscopy (FTIS)

To understand the measured optical absorption spectra, the working principle of FTIS requires introduction. The experimental setup, which can be seen in figure 3.1, includes an IR light source, a Michelson interferometer with the respective mirrors and beam splitter, as well as the sample holder for the sample and a detector [56]. The measurement delivers an Interferogram which is then Fourier-transformed into a spectrum.

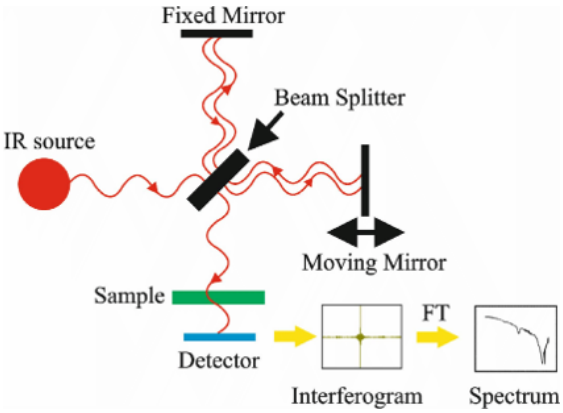

Figure 3.1: Fourier Transform Infrared Spectroscopy working principle taken from [56].

First, the Michelson interferometer is illuminated with a white or polychromatic source of radiation [37]. Depending on the required resolution, the movable mirror is translated over a distance (-L,L). The outgoing beam is passed through a sample which results in an interferogram signal. This is then received by an IR detector. The signal produced by the detector is sampled at certain increments of the intensity in dependency of the mirror displacement $I(\delta)$. The spectrum $S(\nu)$ is recovered from $I(\delta)$ using the real part of the integral transform. To retrieve the characteristic spectrum of the sample, the difference of two spectra $S_i(\nu)$ measurements, one measurement with and one without the sample (background measurement), is taken [37].

3.1.1 SWCNT Samples

The aim of the data collection was to measure OA of different samples of SWCNTs whose chirality was already known, provided by Hiromichi Kataura (in short Kataura samples). As a primary step, three chirality sorted SWCNTs Kataura samples were selected for measurement. These included the chiralities (9,1), (9,2), and (6,5). Due to the high precision and accuracy of the measurements performed with the samples, the data can serve as a reliable foundation for theoretical models [41], which is especially interesting for a future sonification tool development.

3.1.2 Measurements

Due to storage, the samples were dried out and needed to be put back in solution before mounting into the FTIS. SDS (Sodium dodecyl sulfate) was utilized as a surfactant to dilute the SWCNTs, which were then put in an Ultrasonic bath for 5 minutes. The solution was then transferred into a quartz glass with Aluminum strips on the sides. The use of quartz assures that no radiation gets absorbed by the glass. The Aluminum strips ensure that the light bundles not entering through the center of the quartz get reflected.

Preparatory steps on the FTIS before the measurement included the opening of the valve beneath the device and the subsequent evacuation of the system. Before starting the measurement, it was ensured that the correct laser as well as beam splitter were mounted in the device. Only then the sample was installed inside the chamber. For the installation, the sample is placed in a way that the light is most focused when hitting the sample. Therefore it is verified that there is no reflection of the light visible on the Aluminum. After checking the above, the line shapes in the corresponding computer program were checked. The first measurement, however, was the measurement of the background, which was subtracted from the other measurements. After the measurement, the obtained interferogram was converted into a transmission spectrum. This can be directly converted with assistance of the computer program *OPUS* into an absorption spectrum.

3.2 Parameter Mapping Sonification

Parameter mapping sonification represents the most commonly used sonification technique [3]. Through the exploration of the therefore required mapping function, the use of this technique within this thesis has been shown to be the best fit. In order to explain the usefulness of parameter mapping sonification for this application, the following examples should not only explain the mapping function, but will guide towards an understanding for the choice of this technique.

3.2.1 Parking Car

One sonification example from everyday's life, is the beeping sound a car emits when reversing into a parking spot. The idea here is to design a sonification that informs the

driver of the car about the distance between car and back wall when wanting to park the car. Therefore, the closer the car is to approaching the wall, the more alarming the sound is supposed to be. The function of the sound in this scenario includes that no sound should be heard if the car is at a distance greater than 3 m towards the wall. When the distance is less than 3 m but greater than 30 cm the sound should inform the driver about the change in distance. If the car approaches the wall $<$ 30 cm or shorter, the sound should alarm the driver. Figure 3.2 represents the idea graphically. For this sonification,

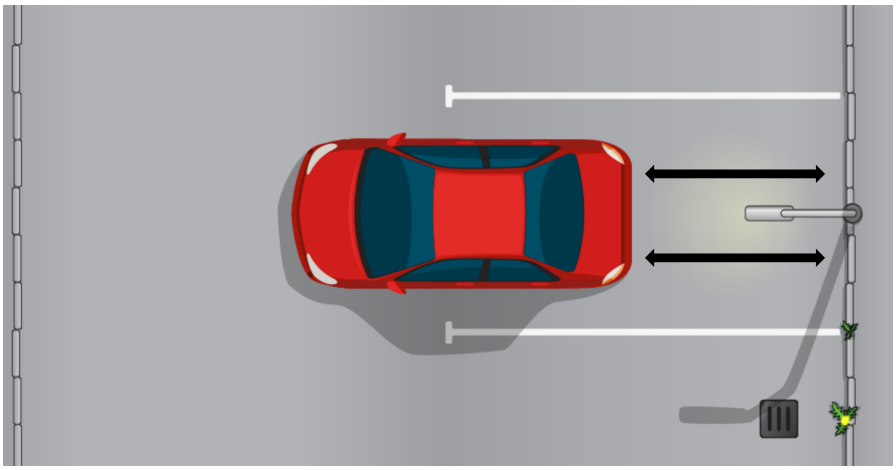

Figure 3.2: Illustration of a car that is in the process of reversing into a parking slot. The black arrows reflect the distance between the car and the wall, which is sonified with an appropriate parameter mapping. Graphic adapted from [57].

parameter mapping sonification was chosen together with the programming environment *SuperCollider*. In this example two parameters were mapped and reflect the information auditively. In *SuperCollider* there are two options how to map the parameters, either linearly or exponentially. The frequency as well as the tempo are mapped exponentially in this example. This means, the closer the car gets to the wall the faster (exponentially) the changes in sound are noticeable. The beeping sound is created in a so-called "SynthDef" using a triangle wave multiplied with a square wave.

```
1 frequency = distance.linexp(0,300,2200,100);
2 tempo = distance.linexp(0,300,5,0.5);
```

The mapping of the frequency explains that the distance, which can lie between 0 and 300 cm, is mapped to a frequency that changes in the range between 2200 and 100 Hz. This means, the closer the car is to the wall, the higher the pitch of the sound gets. The tempo also causes the sound to occur more frequently the closer the car is situated to the wall.

3.2.2 Weather Forecast

In a further example, weather should be sonified using sounds that are generated by artificial intelligence as a foundation, that should then be procedurally adjusted and customized. The sound should represent the temperature, ranging from -20 °C to 40 °C, as well as three different weather conditions (sunshine, rain, and snowfall). The end-product aims to be a soundscape that provides the user with enough information to understand the current outdoor conditions. Figure 3.3 presents a graphical user interface (GUI) which contains a slider bar for different temperatures as well as the three different weather conditions.

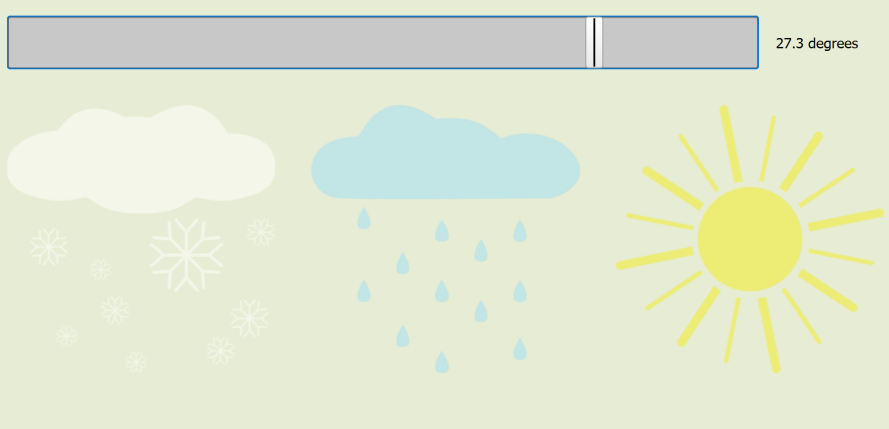

Figure 3.3: Graphical interface [57] where the temperature can be adjusted on the top bar in the range of -20 °C and 40 °C. When clicking on the snow, rain, sun respectively, the weather condition can be selected.

Due to the several parameters that require consideration, this example has several mapping functions. First of all three different sounds are assigned to the weather conditions, each holding sound characteristics for the individual condition, for example sunny weather might be reflected with birds chirping and bees humming, whereas rain could be reflected by the sound of falling rain on forest terrain, while for snow, the sound might reflect a person stomping through snow.

The temperature is divided into three sections, section one ranging from -20 °C until 0 °C, section two ranging from 0 °C until 20 °C and section three ranging from 20 °C until 40 °C. Each section is assigned a different piano melody that reflects the temperature. In section one the piano sounds are low and hammering chords, in section two a beautiful melody is being played and in section three the piano sounds are getting high in frequency. The sounds should function as an information, whether it is too cold or too hot, which can pose a health hazard for people. The sounds are individually mapped in their sound level. Louder again reflects more alarming weather condition, while smooth and more quiet sound level reflect comfortable temperatures.

3.3 Data Processing

The computer program *OPUS*, attached to the FTIS, outputs the absorption spectra in text files with two columns. One column (x-values) represents the wavenumber in [cm^{-1}], while the other column (y-values) shows the intensity values in the range $0 - 1$. In a first step, the data was plotted in *Python* to determine the two characteristic peaks for the energy transition E_{11} and E_{22}. To be able to consider the narrowest range of data in which the peaks appear, subsequently acquired data files only considered the wavenumber range between 8500 cm^{-1} and 18500 cm^{-1}, and the respective intensity values. As each SWCNT chirality shows a unique set of absorption peaks that correlate with the van Hove singularities or kinks in the DOS, the maximum values of the energy transitions E_{11} and E_{22} can be used as orientation points for distinction between the data sets.

The final product of the sonification aims to retrieve an auditive distinction of the individual semiconducting SWCNT chiralities. However, this goal is not trivial to achieve for many reasons, which is why the goal of this thesis is to render first sound files of the measured chirality samples, analyze their respective sonification and suggest how further adjustments and developments can lead to one or multiple suitable sonification designs for B/VI researchers. Different approaches were investigated, considering different parameter mapping techniques. The requirements for the sonification include the consideration of complexity of the obtained sound paired with a non-compulsory requirement of prior musical training.

The first step towards the sonification design approaches the sonification of only the intensity curve (y-values). Due to the attempt to mitigate complexity other data dimensions (wavenumber) are neglected for all following approaches. They can, however, be included in future research directions.

3.4 Isomorphic Approach using MIDI Notes

In the first approach the goal was to retrieve an isomorphic representation of the acquired optical absorption spectra. For this sonification, mapping the data points to MIDI notes was used. To get an audible impression of the course of the spectrum not every data point is necessary. In addition, the limited amount of MIDI notes requires a compression of the data points, otherwise resulting in an overflow error. Therefore the amount of data points is reduced and only every 100^{th} data point is regarded for the mapping. MIDI notes refer to the classical western music scale, which notes are numbered from 0 to 127. Each number has an assigned note, theoretically ranging from C_0 to G_{10}, which extends the piano note range. The corresponding frequencies of the individual notes range from approximately 8 Hz to 12500 Hz. As the human hearing can distinguish different notes best in the range of $250 - 4000$ Hz [47], the range used in the implemented code is adjusted accordingly. In the code, "audiolazy", a *Python* package for signal processing, is used along with a mapping function, that allows the mapping the MIDI notes to the data points. After the definition of the MIDI notes, which range over 9 octaves (from C_0 until C_8), the rendering of the sound files is possible.

The resulting MIDI note mapping can be plotted into a graph of MIDI notes over time, which introduces a second dimension (MIDI notes vs. time).

As mentioned before, there is a limit to the amount of different MIDI notes, hence the amount of unique data points that can be mapped depends on this limitation. To evade such limits, the use of sine notes, to render an isomorphic representation of the intensity curve, is applied in the standard frequency approach, which is described next.

3.5 Standard Frequency Approach

Here, the introduction of a defined standard frequency f_{st} is necessary. To obtain a sonification with frequencies located roughly in the middle of the audible range, different standard frequencies were tested including 880 Hz, 4400 Hz and 8800 Hz. The multiplication of the standard frequency with the individual intensity values (y-values) that range from zero to one will determine a range from 0 Hz to 880/4400/8800 Hz in which all sound frequencies of the individual chiralities will lie.

$$f_i = f_{st} \cdot y_i \tag{3.1}$$

In a next step, sine notes are constructed using the calculated frequency values f_i together with the following expression

$$sinetone = A \cdot sin(2\pi f_i t), \tag{3.2}$$

where A represents the volume in dB, f_i refers to the frequency considered at the individual data point and t denotes the time, resulting in the simplified formulation

$$sinetone = sin(2\pi f_i t). \tag{3.3}$$

When playing the sound file of the resulting sine waves, the individual sine tones are being played at the same time. To be able to hear an individual note for every data point, the sine waves need to be played in a concatenated way. After this adjustment, the tones are played consecutively aiming to represent the positive and negative inclinations of the curve. Ascending tones would thus refer to a positive inclination of the curve, and descending tones to a negative inclination, respectively.

3.6 Earcons Approach

In this approach we consider a basic frequency spectrum, which represents a frequency (y-axis) with a time domain (x-axis), depicted in figure 3.4. Individual frequencies can be graphically represented using their amplitude (y-axis) versus their frequency (x-axis). This shows resemblance to the measured optical absorption spectra where the intensity (amplitude) is represented in dependence of the wavenumber (frequency). Through this consideration, the idea for earcons emerges. Whenever energy transitions (E_{ii}) reach a (local) maximum, the respective intensity value is translated into a note, which is

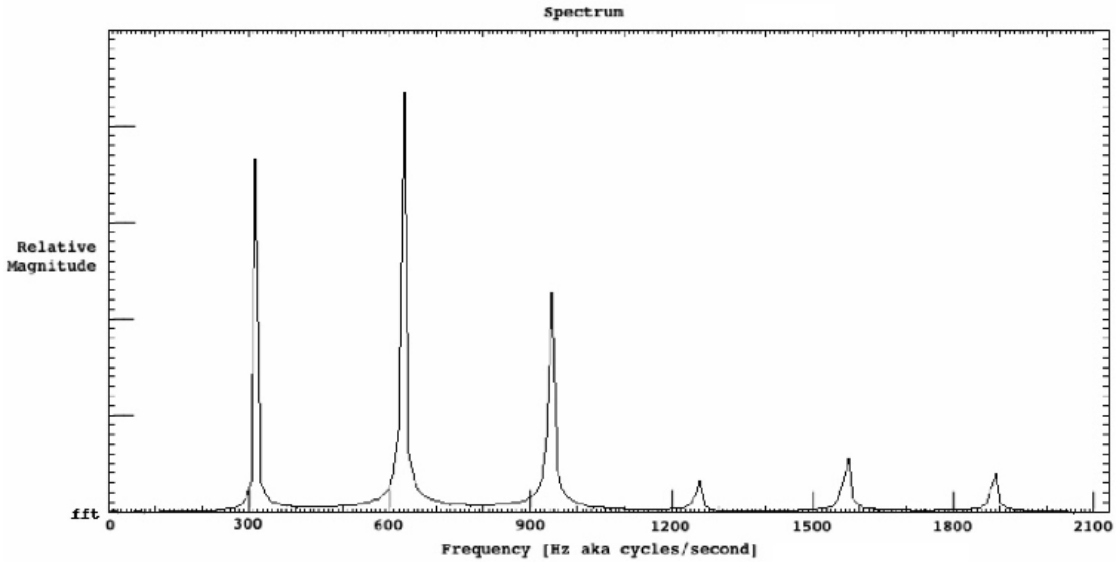

Figure 3.4: Example of an amplitude spectrum of single notes [58].

generated using above mentioned calculation for the standard frequency approach (again testing different standard frequencies: 880 Hz, 4400 Hz, 8800 Hz). In addition, the use of Gaussian fits of the absorption peaks will emphasize the characteristic look of amplitude spectra with which a visual comparison will be possible. The standard description of the Gaussian distribution function is described by

$$f(x) = exp\left(-\frac{(x-\mu)^2}{2\sigma^2}\right), \tag{3.4}$$

where μ is the central value of the distribution and σ its width. This form is used in the numerical implementation. The first two energy transitions will result in two notes representing each chirality. This is being illustrated (visually and audible) by the use of the information retrieved from the Gaussian fits together with the calculated frequency values from the standard frequency approach, which are then plotted into respective amplitude spectra. These can be played either as a chord or consecutively (like a melody). This is the basis to adapt the chords into individual earcons for each set of energy transitions for the different chiralities. In a future project, earcons for all available theoretical energy transitions will be generated. These will then be stored as default values for each available chirality. When a user wants to compare a new measurement to determine its chirality, he will hear the earcon from the library in the left ear and the earcon from the new measurement in the right ear. The comparison of the sounds in the left and right ear has the purpose of enabling the determination of a chirality auditively. However, since some energy transitions are similar or overlapping, the need for another complimentary approach is emphasized.

4 Results

In order to answer the research questions introduced in the first chapter, this section will unite the knowledge gathered about the physics of SWCNTs and will bridge the connection to the sonification approaches. The discussion will suggest how different approaches and angles on this project have the potential to greatly influence the sonification choices and respective designs developed in the future. For retrieving the individual sound files please contact the author.

4.1 Optical Absorption Spectra

The resulting optical absorption spectra for chiralities (9,1), (9,2) and (6,5) are represented in 4.1, showing the intensity in dependency of the wavenumber in [cm^{-1}]. The theoretical energy transition values can be extracted [41] and compared with the measured values. Table 4.1 provides the values for the energy transitions at the respective wavenumber in

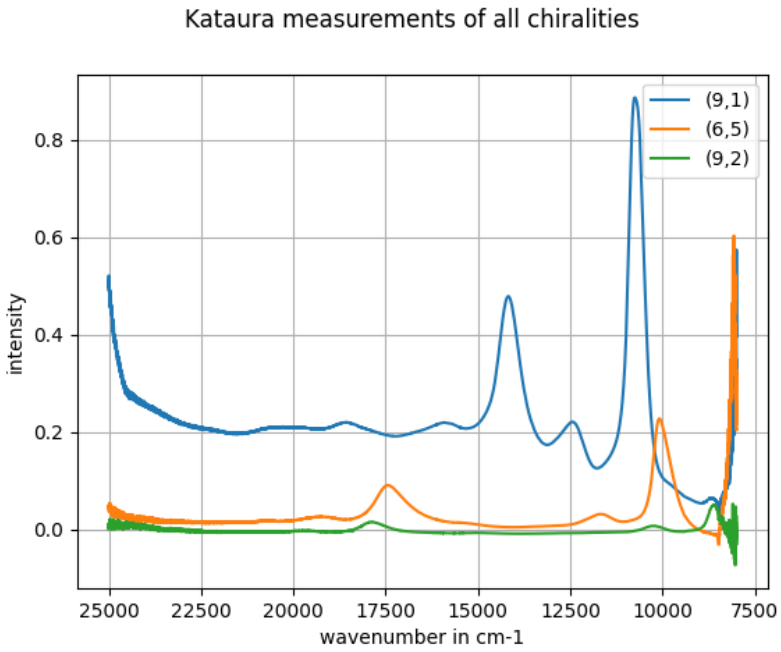

Figure 4.1: Measured optical absorption spectra for the SWCNT chiralities (9,1), (9,2) and (6,5).

[cm^{-1}] both, theoretical and empirical.

(n,m)	$E_{11,theoretical}$	$E_{11,empirical}$	$E_{22,theoretical}$	$E_{22,empirical}$
(9,1)	$10964cm^{-1}$	$10752cm^{-1}$	$14466cm^{-1}$	$14184cm^{-1}$
(9,2)	$8790cm^{-1}$	$8606cm^{-1}$	$18155cm^{-1}$	$17861cm^{-1}$
(6,5)	$10244cm^{-1}$	$10086cm^{-1}$	$17667cm^{-1}$	$17347cm^{-1}$

Table 4.1: Comparison between theoretical [41] and empirical values for the wavenumber in $[cm^{-1}]$ where the local maxima of the respective energy transition appears.

The values stand in fair agreement with the theoretical values, deviating from each other by only $1,5\% - 2,1\%$. Overall, the range in which the peaks of the absorption spectrum are located lies between 8500 cm^{-1} and 18500 cm^{-1}, which enables a slicing of the data above and below this range.

4.2 Isomorphic Approach

Figures 4.2, 4.3 and 4.4 represent the OA spectra of the three chiralities in the wavenumber range 8500 cm^{-1} and 18500 cm^{-1} with a compression factor of 100. As mentioned in chapter 3, the compression is necessary to prevent an overflow of the MIDI notes. However, as the goal of this sonification is to get an impression of the isomorphic course of the spectra, it is not necessary to use all data points for the sonification anyway.

While the left graphs show the OA measurements (intensity over wavenumber), the right graphs show the MIDI note values for the individual data points (MIDI number over time) ranging from C_0 (MIDI note number 24) until C_8 (MIDI note number 120).

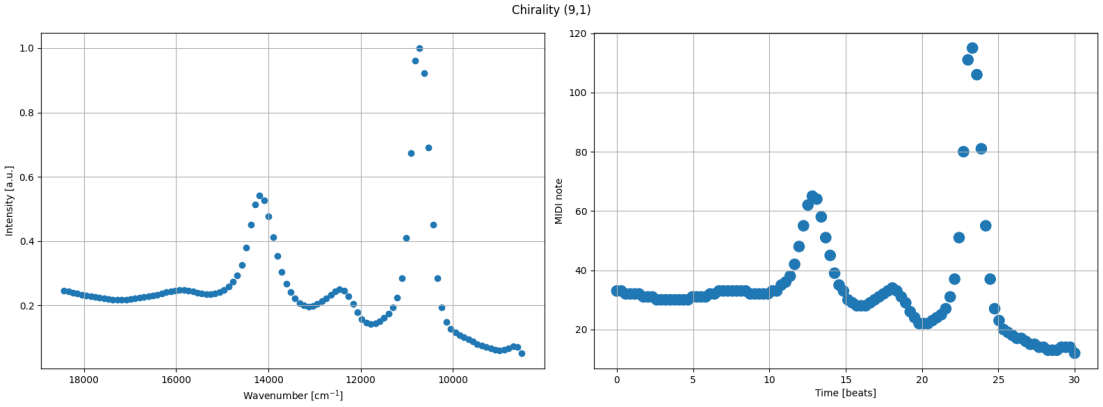

Figure 4.2: Comparison of the optical absorption spectrum of (9,1) considering only every 100^{th} data point (left) and the respective representation of this data with MIDI notes (right).

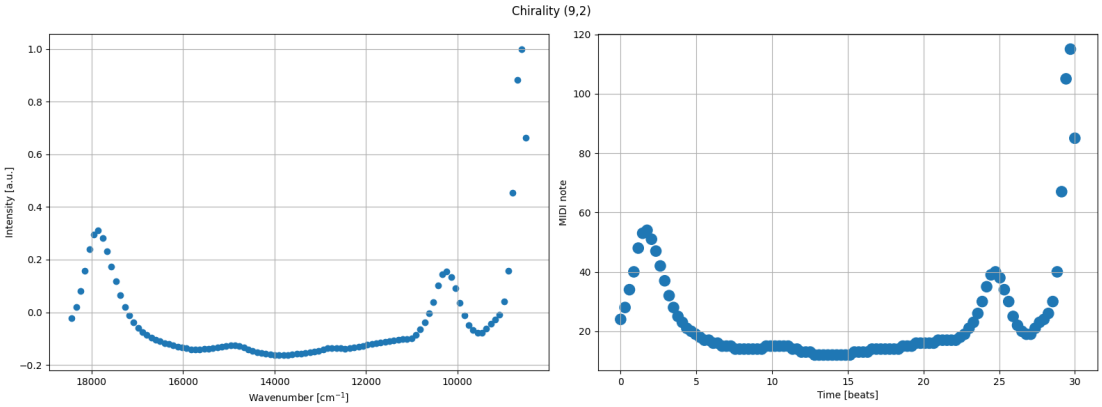

Figure 4.3: Comparison of the optical absorption spectrum of (9,2) considering only every 100^{th} data point (left) and the respective representation of this data with MIDI notes (right).

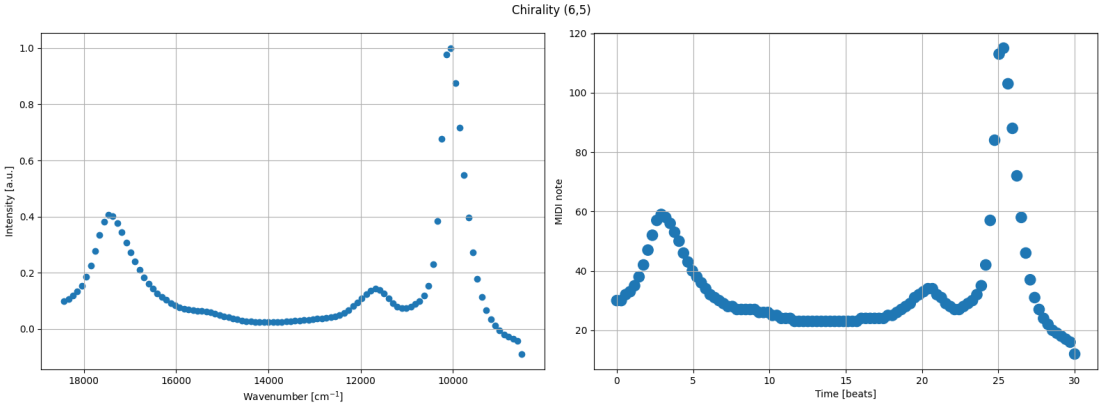

Figure 4.4: Comparison of the optical absorption spectrum of (6,5) considering only every 100^{th} data point (left) and the respective representation of this data with MIDI notes (right).

4.3 Standard Frequency Approach

The graphical results of the sound files of this approach can be seen in Figures 4.5, 4.6 and 4.7. Left graphs again show the OA measurements for the individual chiralities (intensity over wavenumber), while the right graphs depict the oscillations of the individual sine notes for each data point (amplitude over time).

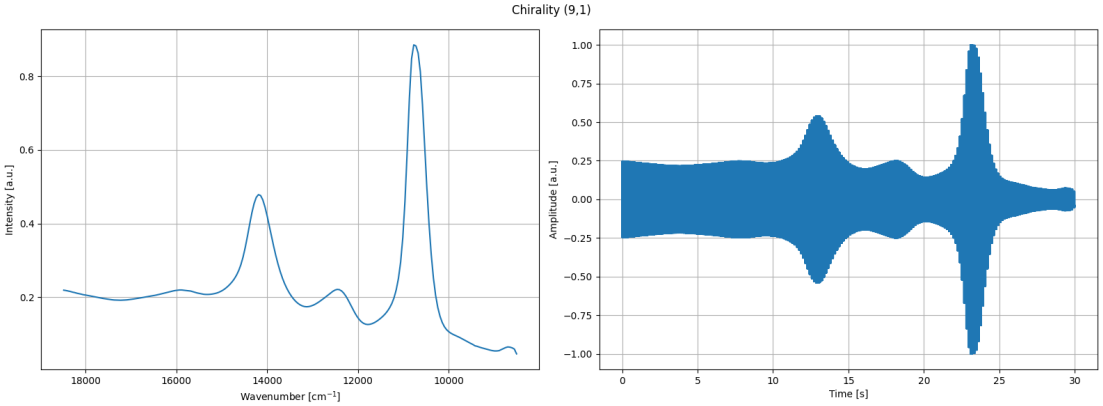

Figure 4.5: Comparison of the optical absorption spectrum of (9,1) (left) and the respective representation of the different concatenated frequencies of the standard frequency approach (right).

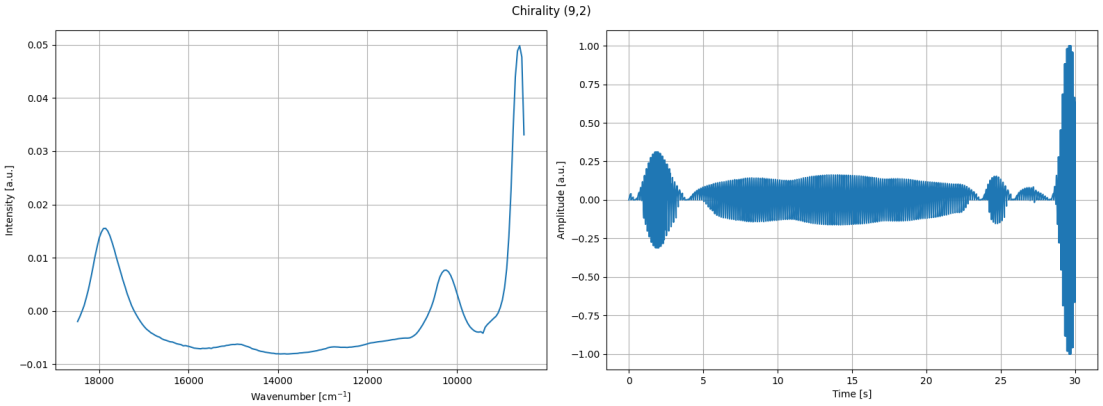

Figure 4.6: Comparison of the optical absorption spectrum of (9,2) (left) and the respective representation of the different concatenated frequencies of the standard frequency approach (right).

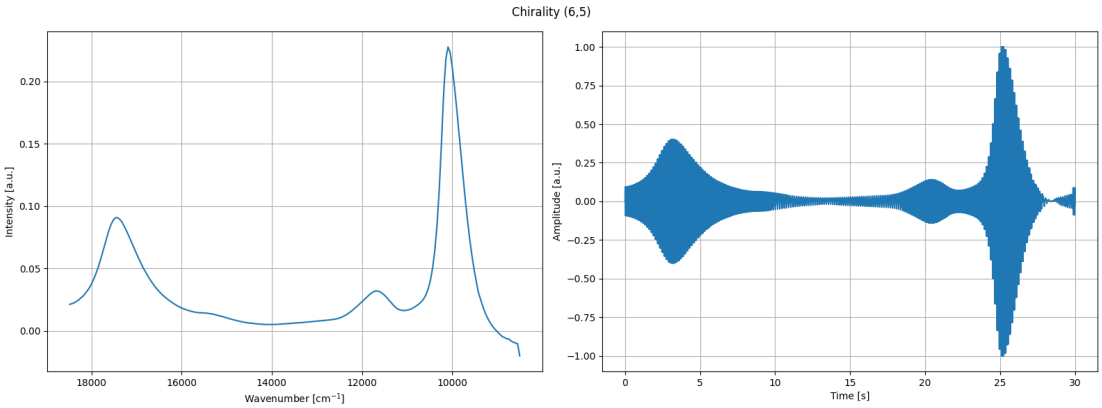

Figure 4.7: Comparison of the optical absorption spectrum of (6,5) (left) and the respective representation of the different concatenated frequencies of the standard frequency approach (right).

4.4 Earcons Approach

Gaussian fits are used to approximate the absorption spectra to be able to retrieve normal distributed maxima values, the fits are depicted on the left side of Figures 4.8, 4.9 and 4.10. The right sides show the frequency peaks determined on the basis of the Gaussian peaks together with the calculated frequency values at the respective intensity value from the standard frequency approach and the optics of an amplitude spectrum (see figure 3.4). Usually the axis of amplitude spectra are amplitude on the y-axis and frequency on the x-axis. The output are two tones (as described in chapter 3) and the graph should visually represent what one hears in the sound files (change of frequencies and not change in amplitude and frequency).

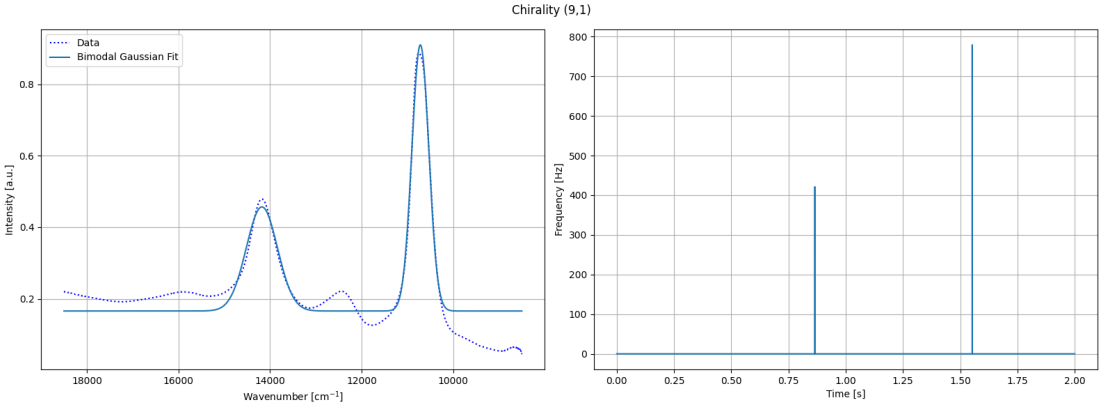

Figure 4.8: Gaussian fits of the two characteristic energy transition peaks of the optical absorption spectrum of (9,1) (left) and the according graphical representation of the Earcon Approach (right). Standard frequency 880 Hz and compression of 1.

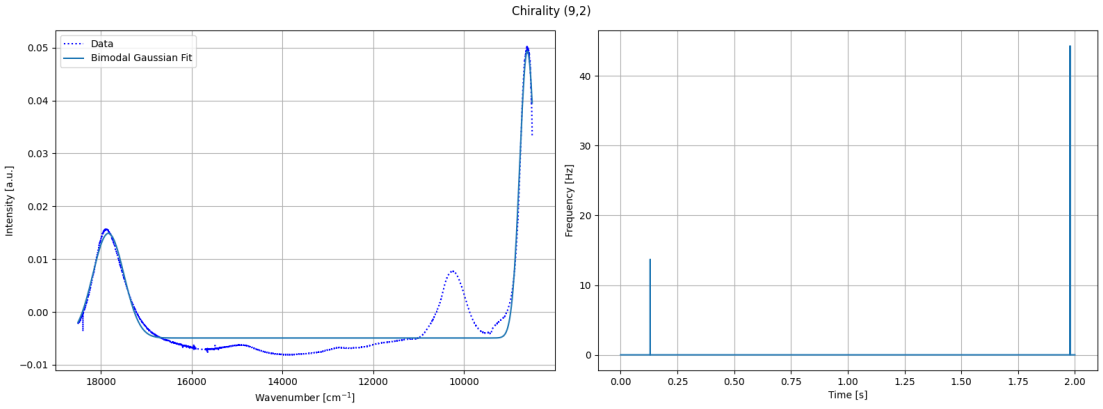

Figure 4.9: Gaussian fits of the two characteristic energy transition peaks of the optical absorption spectrum of (9,2) (left) and the according graphical representation of the Earcon Approach (right). Standard frequency 880 Hz and compression of 1.

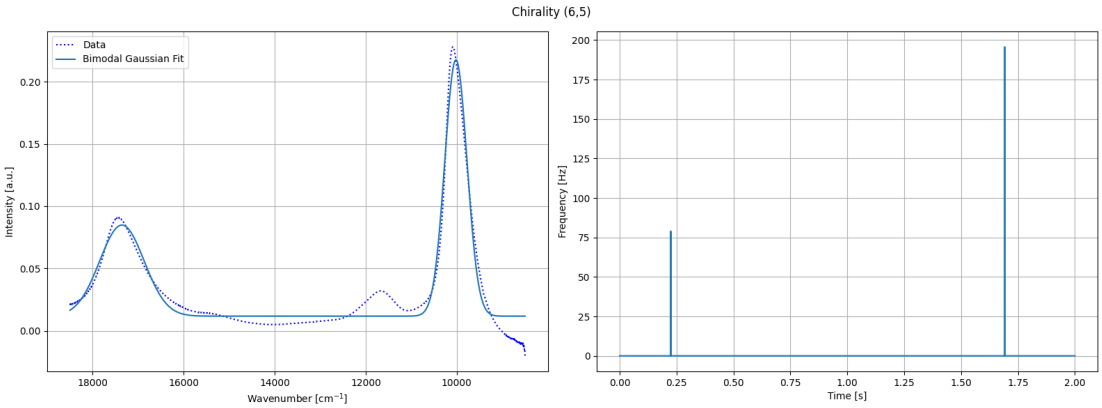

Figure 4.10: Gaussian fits of the two characteristic energy transition peaks of the optical absorption spectrum of (6,5) (left) and the according graphical representation of the Earcon Approach (right). Standard frequency 880 Hz and compression of 1.

The notes lie in the range of $0Hz$ to $880Hz$ which produces mainly audible clicks instead of tones. Therefore different compression factors and standard frequencies are tested. The spectra of these trials can be seen in figure 4.11 and 4.12.

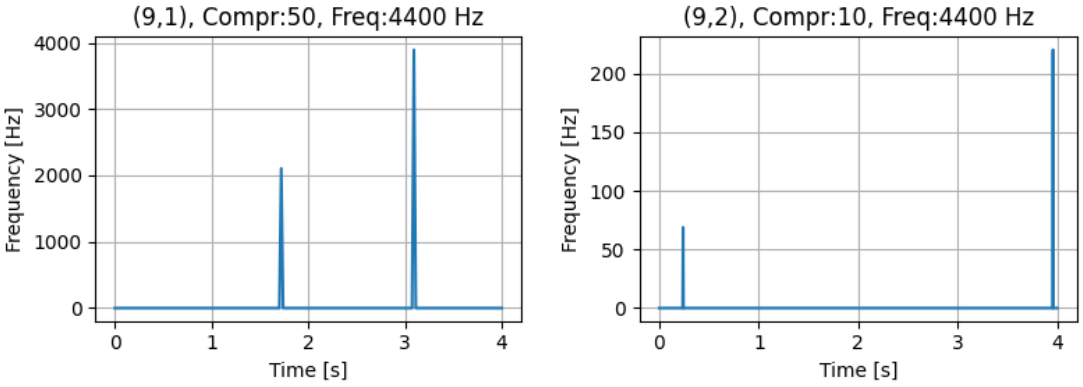

Figure 4.11: Left: (9,1) earcon spectrum with compression of 50 and standard frequency of 4400 Hz. Right: (9,2) earcon spectrum with compression of 10 and standard frequency of 4400 Hz.

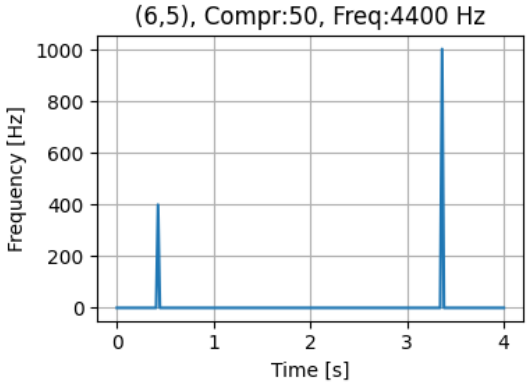

Figure 4.12: (6,5) earcon spectrum with compression of 50 and standard frequency of 4400 Hz.

5 Discussion

The results show that the absorption peaks in the measurements all lie in the range between 8500 cm^{-1} and 18500 cm^{-1}, which justifies the filtering of the data below and above this range. Comparing the different approaches poses a variety of different aspects that require discussion.

To start with, a few words about the sound choices. As mentioned in the theory background (chapter 2), depending on the project and its sonification goal, the sounds can either be informative (e.g. alarming, explaining data, etc.) or non-informative (e.g. musical composition). Depending on the function the kind of sounds, that can either be aesthetic, including rather harmonic and melodic components or unaesthetic including noisy and distorted sounds, needs to be determined. This choice shapes the listening experience of the listener by making it either more comfortable or uncomfortable. As the goal of this project targets the distinction of different chiralities through sound, the requirements for the sound design are to be simple and "nice" for the listener. This means that the frequency of the pitch is not too high as well as using sine waves and MIDI notes, which provide a smoother listening experience.

The concept for the sonification oriented itself on the three research questions posed in the beginning of this thesis. First of all, the optical absorption spectra, which reflect the interaction between photons and SWCNTs (optical properties), were analyzed. The sonification was achieved through the use of the respective energy transition peaks in the optical absorption spectra of measured chiralities, as they appear at characteristic wavenumbers for individual SWCNTs. As the knowledge of the the chirality allows understanding about the individual nanotube behavior, it was decided to use this as the parameter or property for sonification.

Secondly, the sound design for these peaks was approached with different concepts. The isomorphic approach, the standard frequency approach and the earcons approach present different approaches how sonification sounds can be rendered.

The first approach targets a sound rendering which follows the identical path of the absorption spectrum. This was attempted by mapping MIDI notes to the data range. As the range of the data is bigger than the available number of MIDI notes, the data needs to be compressed at least by a factor of 100. The sound files, which have all a similar length of 30 s, are giving the listener an impression about the course of the data (ascending notes mean positive inclination and descending notes mean negative inclination).

In order to sonify each data point without compression, the next approach sonified the data using sine tones. This approach was refined using a standard frequency which is multiplied by the intensity values. Consecutive sine tones were created, resulting in a normalization of the note ranges and therefore ensuring a more scientific comparability in between data sets. Different standard frequencies are tested, as too low intensities with a

standard frequency $f_{st} = 880$ Hz results in ill-distinguishable clicking noises. On the other hand, a standard frequency that is too high, $f_{st} = 8800$ Hz can lead to very high notes at peaks approaching an intensity of 1, resulting in an uncomfortable listening experience. However, as the sound files have the length of 30 s, the comparison of different chirality sonifications for the user is challenging, especially without prior musical training, which is why in the third approach this complexity is mitigated through earcons.

Earcons have the potential to transmit key information of the data which can assist in identifying features or patterns in the data [59]. As the sounds of earcons are usually short (only a few seconds) the attention of the listener can easily be directed. Therefore the use of earcons within this project emerges. Chords could be assigned to the individual chiralities, based on the resemblance of an amplitude spectrum. These earcons provide the basis for a library in which the sounds for each chirality can be stored and summoned on demand. When a B/VI researcher needs to figure out the chirality of a newly measurement spectrum, the idea is that the stored sonification is played at one ear and the new measurement is simultaneously played in the other ear. Either the sounds match or the sounds differ, which will be audible through beating, or different intervals. Through this, the determination of the chirality should be possible.

Thirdly, the answer for the question which parameter mappings would represent an appropriate fit for the optical properties is not trivial. All approaches emphasize how these spectra can be sonified in a first attempt. The earcons approach has the potential to represent an appropriate parameter mapping sonification. However, to be able to apply these approaches on a large amount of different data sets, many aspects still require attention and recognition. As in this case, datasets of the energy transitions of about 220 different chiralities are available [41], resulting in 220 different earcons. Remembering all individual earcons to be able to make an audible distinction is fairly unreasonable. Therefore, a way of systematically browsing the earcons would need to be established.

Claims about the validity and reliability of this project need elaboration. This work demonstrates first attempts towards an auditive interpretation of optical absorption spectra of selected chiralities of semiconducting SWCNTs. This, however does not mean that the constructed approaches are complete. This thesis attempts to cover the theory of two different matters which are aimed to be connected. The validation and choice of which approach is better suited compared to the others, is based on directly testing and analyzing the sound files and by weighing which rendered sounds might be too complex. Based on these personal proofs of concept, together with the developed theoretical knowledge, first approaches towards answering the research questions were implemented. However, the necessity of assessments together with experts and testing as well as review of the approaches together with scientists, both with and without visual impairments, is undisputed.

Moreover, the first priority of this thesis was the introduction of sonification into solid state physics. The definition of a target group assisted in shaping the design choices of the sonification approaches. It however did not lead to an extensive study of the needs of B/VI researcher for this sonification design, which is why future development requires a strong examination of their needs. The different sonification approaches aim to benefit the

user in exploring the data. The evaluation of the approaches and their claims about their suitability were made by a user with normal visual acuity, stating that this sonification would most probably also support visually impaired users in their work.

5.1 Requirements B/VI Researcher

As the world population grows daily, so does the number of people living with impairments. Especially the number of those affected by vision impairments, spanning from blindness to minor impairments and psychological impairments including dyslexia, etc., rises steadily. The number of researchers with some kind of vision impairment or psychological impairments worldwide that face challenges in the accessibility of data analysis is unknown [1]. Sonification provides an interdisciplinary approach which holds the potential to address the still existing accessibility issues. Sound can be seen as an audible visualization technique that can assist in interpreting and analyzing data of different kinds. Sonification is the translation of data into sounds and can therefore be used to create not only (sound) tools but different means of how data can be visualized using sound. This thesis tries to approach on one hand the data exploration of OA spectra of different chiralities of semiconducting SWCNTs with sonification with the goal on the other hand to provide more accessibility to B/VI researcher. For further development of the introduced concepts, the awareness for the needs and requirements of B/VI researcher need to be addressed and strengthened more. Several aspects, including the different perceptions of sound, how data is conveyed and which tools are used so far for data analysis, need recognition. In addition to a thorough literature research, user studies including the testing of different approaches need to be conducted.

5.2 Further Research Trajectories

Sonification poses a research field with which accessibility and inclusivity can be addressed. Using sound as a medium to represent data can not only lower the barriers for B/VI researcher, but it can also assist researcher to create more inclusive ways of presenting scientific information [60]. Whether it is for exploration and understanding data as a scientist or for communicating data and research in form of a public outreach activity. The early stages of this project still allow to apply different sonification strategies and to also explore other targets and audiences such as aiming for a public outreach activity, which can be paired with the sonification for the B/VI researcher.

5.2.1 Color Approach

The discussed research towards the sonification of elemental spectra in the background chapter [47], acts as basis for this approach, which is, however, only of theoretical nature so far.

Usually, the visible light waves range from 750 THz to 420 THz, which is undoubtedly a larger range compared to audible frequencies for the human ear. Scaling down the color

frequencies by a factor between 10^{-11} and 10^{-13} will pull them down into the human hearing range ($20 - 20,000$ Hz) [47].

Through the previously described optical processes that occur in SWCNTs, their color in solution depends on their chirality and diameter. This correlation is described by a quantitative model [24]. However, further experiments need to be conducted to retrieve an experimental color gradient of as many chiralities as possible. Once a pattern for the coloration mechanism of the nanotubes is discovered the respective sonification concept can be implemented. Therefore the above mentioned publication [47] acts a the basis for this idea. The different colors of SWCNTs can each be assigned a distinctive note or even earcon in a further step, which should result in a method that complements the other sonification approaches mentioned for the auditive distinction of different SWCNT chiralities.

5.2.2 Browsing Design

To be able to apply the earcons approach on a large dataset, the introduction of a browsing system is necessary. A step by step data sonification should explore the data in different layers, with future possibilities of even designing some kind of interaction with which you can scrub through the layers. This idea would include to "slice" the data into different layers. Within the absorption spectra the x-values (wavenumber) can be first split into two sections (in this case range one lies between 8500 cm^{-1} and 13500 cm^{-1} and range two from 13500 cm^{-1} to 18500 cm^{-1}). Each section could have a sound-file playing for 10 seconds, where every second refers to 500 cm^{-1}, as soon as the peak is detected it will produce a sound. For the second section, the same procedure will run. As a result the listener will conclude with the first distinction in which sections the peaks appear (either both in one section or one in each section, additionally the listener is able to analyze whether the sound is rather in the beginning or in the end of the sound files). The next slice is working with the same principle, but this time there are four sections, etc. In each layer, certain chiralities can be excluded from the list and therefore the listener is one step closer in approaching the right chirality. When the listener reaches a reasonable amount (approximately 5-10 chiralities) the earcons approach from this thesis can be used to distinguish which chirality it is. Tool testing should target the reasonability and user friendliness of this approach and answer the question whether a program should scrub through the data bank and look for similar graphs as a first brows instead, which outputs only the most similar ones to the earcons library.

5.2.3 Sonification of Differences in Spectra

The sonification can also be focused in highlighting the differences between the different chiralities. This approach could include the consideration of one initial note, which changes at a rate that is tied to the changes of the peaks of different chiralities. Another idea to this approach could be to subtract different chiralities from each other and sonify either the remaining area or the resulting new line shape of the graph.

5.2.4 Higher Dimensional Data

Tied to the approaches considered in this thesis, a next step could consider more data dimensions of the absorption spectra. The information about the wavenumber can be sonified in addition to the intensity data, to retrieve a 2D representation of the data. A more advanced step would include the sonification of the 3D Photoluminescence spectra. Together with the color sonification, a complete auditive picture of nanotubes could be drawn.

5.2.5 Different Parameter Selection

Lastly, the possibility to consider different parameters for sonifying the optical properties is given. Reflecting about which part of the spectrum is represented auditively, which can either be the frequency or wavenumber, or even the width or the intensity of the peak, opens up a new playground yet to explore.

6 Conclusion and Outlook

In this thesis theoretical aspects of the nature of semiconducting SWCNTs with an emphasis on their optical properties have been studied. Along with that, sonification and its background has been introduced. The interdisciplinary approach to combine these two fields aimed towards an auditive interpretation of optical absorption spectra of selected chiralities of SWCNTs. This was not investigated to full extent as many different aspects of this project brought along diverse problems and difficulties. Unfortunately, not all of them were solvable in the framework of this project. As the research questions imply, a selection of which properties would be sonified and a respective justification for that choice were the main goals of this work.

Using the mapping of MIDI notes to the data points of the intensity of the optical spectra, revealed that the range of the data is bigger than the range of available MIDI notes, resulting in an overflow, which can be fixed by compressing the data. Therefore this approach was then re-implemented using sine notes for the individual data points. To retrieve sound-files, that are comparable in between different data sets, the standard frequency approach targeted the use of multiple standard frequencies, which resulted in a normalization of the tones. As the sound-files still required high prior musical understanding to be able to interpret the sounds, the earcons approach tried to mitigate this complexity. Using the representation of amplitude versus frequency (amplitude spectrum) instead of frequency versus time, gave rise to the idea of assigning chords to the individual SWCNT chiralities, in the form of earcons. The idea of this approach also includes that the listener will hear the tones of the chord in succession on one ear while hearing the just measured sample on the other ear. This should lead to an auditive distinction method for different chiralities. However, as there would be over 200 individual chords, as this is the number of theoretical predicted energy transitions for the individual chiralities, this approach is still too complex for quick data analysis, especially for B/VI researcher. However, the first sound rendering can be used for example to compare the sound of the "theoretical" and "experimental" sound of the same chirality. For that reason further investigations towards a more accessible sonification design, considering the needs and (sound) perception of B/VI researcher is required. The discussion already suggested which parameters require further attention, highlighting the necessity to zoom out of the data and start to approach the sonification design layer by layer.

The results and interpretations presented herein open the door for multiple future research directions, as the individual approaches worked on in this thesis undoubtedly have potential for further investigation. When considering the currently available list of different chiralities and their energy transitions [41] the need of a browsing system for the B/VI is emphasized to handle the big amount of data. Therefore, the wavenumber range could be divided first into two big parts, where a program automatically assigns the

sonification depending on the peaks in the respective absorption spectrum. The second iteration will already have four or more sections into which the spectra are divided. This can be repeated as oftten as necessary until only few different sonifications remain. These can then be compared like suggested in the earcons approach.

The earcons approach can also be further adapted by including more data dimensions of the optical absorption spectra, but also starting to approach photoluminescence spectra. This can ultimately lead to a tool development for carbon nanotube data analysis. Especially when implementing and exploring the color sonification approach. This will contribute for gaining a more complete auditive picture of the physics and properties of carbon nanotubes. As the investigation of the coloration theory still requires some more attention and experimental measurements, this trajectory entails both experimental work and sonification design.

New research could be conducted towards the approach of considering a different selection of parameters of the optical absorption spectra that are being sonified (width of peaks, frequency/wavenumber, intensity, etc.).

Paired with user tests, all approaches lead to highlighting the potential and impact, that these methods have for revolutionizing the way carbon nanotube data is understood so far.

Another benefit of rendering sonifications of the optical absorption spectra represents the opportunity of creating a science communication activity or public outreach for non-scientists. Together with the retrieved sonification outcomes, which either are earcons or parameter mapped sounds, an immersive sound installation together can be planned. Using the sound as one component and a visualization design of a carbon nanotube structure, will allow to present the state of the art research progress in an innovative way.

List of Tables

List of Figures

Glossary

B/VI Blind/Visually Impaired. viii, 1, 23, 36, 37, 41

BZ Brillouin Zone. 9, 10, 45

C Carbon. 3

CB Conduction Band. 3, 7–9, 12

CNT carbon nanotube. 3–6, 9, 11, 17, 43

DOS Density Of States. 5, 7, 9, 11, 23

FTIS Fourier Transform Infrared Spectroscopy
. vii, 13, 19, 20, 23

GaAs Galliumarsenid. 3, 8, 45

HCI Human Computer Interaction. 15

IR Infrared. 13, 17, 19

JDOS Joint Density Of States. 9

MIDI Musical Instrument Digital Interface. vii, 23, 24, 28, 29, 35, 41, 45, 46

MWCNT Multi-walled carbon nanotube. 4, 12, 45

OA Optical Absorption
. 20, 28, 30, 37

OAS Optical Absorption Spectroscopy
. vii, 1, 2, 8, 12–14, 19

PL Photoluminescence. 7, 8, 10

PLS Photoluminescence Spectroscopy. vii, 1, 15

RBM Radial Breathing Mode. 11

SDS Sodium Dodecyl Sulfate. 20

Si Silicium. 3

SWCNT single-walled carbon nanotube. vii, 1–4, 6–12, 14, 15, 17, 19, 20, 23, 27, 35–38, 41, 43, 45

VB Valence Band. 3, 7–9, 12

WHO World Health Organization. 1

ZF Zone Folding. 11

Bibliography

[1] World Health Organization. Blindness and vision impairment, 2023. [Accessed on 23-03-2025]. URL: https://www.who.int/news-room/fact-sheets/detail/blindness-and-visual-impairment.

[2] Vision Loss Expert Group of the Global Burden of Disease Study. Global estimates on the number of people blind or visually impaired by cataract: a meta-analysis from 2000 to 2020. *Eye*, 38(11):2156–2172, March 2024. doi:10.1038/s41433-024-02961-1.

[3] Thomas Hermann, Andy Hunt, and John G Neuhoff, editors. *The Sonification Handbook*. Logos Verlag Berlin, Berlin, Germany, December 2011.

[4] Gaël Dubus and Roberto Bresin. A systematic review of mapping strategies for the sonification of physical quantities. *PLoS ONE*, 8(12):e82491, December 2013. doi:10.1371/journal.pone.0082491.

[5] S. Lenzi, P. Ciuccarelli, H. Liu, and Y. Hua. Data sonification archive, 2020. [Accessed 23-03-2025]. URL: https://sonification.design/.

[6] M Russo and A. Santaguida. Cosmic harmonies: Sonifications from nasa telescopes, 2023. [Accessed 10-04-2025]. URL: https://chandra.si.edu/photo/2023/sonify7/.

[7] Levy Lorenzo. Song of the tides, 2010. [Accessed 10-04-2025]. URL: https://www.math.stonybrook.edu/~tony/tides/venice/ancona3000.html.

[8] Duncan Geere and Miriam Quick. A symphony of bureaucracy by loud numbers, 2021. [Accessed 10-04-2025]. URL: https://creators.spotify.com/pod/profile/loudnumbers/episodes/A-Symphony-of-Bureaucracy-e131ap7.

[9] Takeshi Saito. *Carbon Nanotubes and Graphene*. Elsevier, edition 2 edition, 2014. doi:10.1016/C2011-0-07380-5.

[10] R. Saito, A. Grüneis, G.G. Samsonidze, G. Dresselhaus, M.S. Dresselhaus, A. Jorio, L.G. Canccado, M.A. Pimenta, and A.G. Souza Filho. Optical absorption of graphite and single-wall carbon nanotubes. *Applied Physics A*, 78(8):1099–1105, May 2004. doi:10.1007/s00339-003-2459-z.

[11] Mercè Pacios Pujadó. *Carbon Nanotubes as Platforms for Biosensors with Electrochemical and Electronic Transduction*. Springer Berlin Heidelberg, 2012. doi:10.1007/978-3-642-31421-6.

[12] E. Velmre. Thomas johann seebeck (1770–1831). *Estonian Journal of Engineering*, 13(4):276, 2007. doi:10.3176/eng.2007.4.02.

[13] G. Busch. Early history of the physics and chemistry of semiconductors-from doubts to fact in a hundred years. *European Journal of Physics*, 10(4):254–264, October 1989. doi:10.1088/0143-0807/10/4/002.

[14] Peter Y. Yu and Manuel Cardona. *Fundamentals of Semiconductors: Physics and Materials Properties*. Springer Berlin Heidelberg, 2010. URL: http://dx.doi.org/10.1007/978-3-642-00710-1, doi:10.1007/978-3-642-00710-1.

[15] Y. Iye. 1.10 - electronic states and transport properties of carbon crystalline: Graphene, nanotube, and graphite. In Pallab Bhattacharya, Roberto Fornari, and Hiroshi Kamimura, editors, *Comprehensive Semiconductor Science and Technology*, pages 359–382. Elsevier, Amsterdam, 2011. doi:10.1016/B978-0-44-453153-7.00068-7.

[16] Marc Monthioux and Vladimir L. Kuznetsov. Who should be given the credit for the discovery of carbon nanotubes? *Carbon*, 44(9):1621–1623, August 2006. doi:10.1016/j.carbon.2006.03.019.

[17] Marina Filchakova and Vladimir Saik. Single-walled carbon nanotubes: structure, properties, applications, and health & safety, 2021. [Accessed on 21-03-2025]. URL: https://tuball.com/articles/single-walled-carbon-nanotubes.

[18] R. Saito, G. Dresselhaus, and M. S. Dresselhaus. *Physical Properties of Carbon Nanotubes*. Imperial College Press, July 1998. doi:10.1142/p080.

[19] Silvia Zecchi, Giovanni Cristoforo, Erik Piatti, Daniele Torsello, Gianluca Ghigo, Alberto Tagliaferro, Carlo Rosso, and Mattia Bartoli. A concise review of recent advancements in carbon nanotubes for aerospace applications. *Micromachines*, 16(1):53, December 2024. doi:10.3390/mi16010053.

[20] Thomas J. Sisto, Lev N. Zakharov, Brittany M. White, and Ramesh Jasti. Towards pi-extended cycloparaphenylenes as seeds for cnt growth: investigating strain relieving ring-openings and rearrangements. *Chemical Science*, 7(6):3681–3688, 2016. doi:10.1039/c5sc04218f.

[21] Feng Yang, Meng Wang, Daqi Zhang, Juan Yang, Ming Zheng, and Yan Li. Chirality pure carbon nanotubes: Growth, sorting, and characterization. *Chemical Reviews*, 120(5):2693–2758, February 2020. doi:10.1021/acs.chemrev.9b00835.

[22] Marziyeh Karandish, Somayeh Fardindoost, and Gholamreza Pazuki. A novel approach in sorting chirality species of single-wall carbon nanotubes based on an aqueous two-phase system of polymer-salt. *Scientific Reports*, 10(1), February 2020. doi:10.1038/s41598-020-58993-6.

[23] Jean-Christophe Charlier, Xavier Blase, and Stephan Roche. Electronic and transport properties of nanotubes. *Reviews of Modern Physics*, 79(2):677–732, May 2007. doi:10.1103/revmodphys.79.677.

[24] Nan Wei, Ying Tian, Yongping Liao, Natsumi Komatsu, Weilu Gao, Alina Lyuleeva-Husemann, Qiang Zhang, Aqeel Hussain, Er-Xiong Ding, Fengrui Yao, Janne Halme, Kaihui Liu, Junichiro Kono, Hua Jiang, and Esko I. Kauppinen. Colors of single-wall carbon nanotubes. *Advanced Materials*, 33(8), December 2020. doi:10.1002/adma.202006395.

[25] Hiroshi Ajiki. Exciton states and optical properties of carbon nanotubes. *Journal of Physics: Condensed Matter*, 24(48):483001, November 2012. doi:10.1088/0953-8984/24/48/483001.

[26] M. R. Shenoy. Absorption spectrum of semiconductor, 2013. Department of Physics, IIT Delhi, [Accessed on 02-04-2025]. URL: https://youtu.be/zZInsuCpra8?feature=shared.

[27] Pavel V. Avramov, Konstantin N. Kudin, and Gustavo E. Scuseria. Single wall carbon nanotubes density of states: comparison of experiment and theory. *Chemical Physics Letters*, 370(5–6):597–601, March 2003. doi:10.1016/s0009-2614(03)00113-1.

[28] R. Bruce Wiseman and Shekhar Subramoney. Carbon nanotubes. *The Electrochemical Society Interface*, 15(2):42, June 2006. doi:10.1149/2.F06062IF.

[29] Masahiro Nomura, Roman Anufriev, Zhongwei Zhang, Jeremie Maire, Yangyu Guo, Ryoto Yanagisawa, and Sebastian Volz. Review of thermal transport in phononic crystals. *Materials Today Physics*, 22:100613, January 2022. doi:10.1016/j.mtphys.2022.100613.

[30] K.G. Nakamura. *Coherent Control of Optical Phonons in Solids*, page 334–337. Elsevier, 2018. doi:10.1016/b978-0-12-409547-2.13236-6.

[31] David Tuschel. Why are the raman spectra of crystalline and amorphous solids different? *Spectroscopy*, 32:26–33, March 2017. URL: https://www.spectroscopyonline.com/view/why-are-raman-spectra-crystalline-and-amorphous-solids-different.

[32] Rasmita Sahoo and Rashmi Ranjan Mishra. Phonon dispersion for armchair and zigzag carbon nanotubes. *Graphene*, 03(02):14–19, 2014. doi:10.4236/graphene.2014.32003.

[33] J.-L Sauvajol, E Anglaret, S Rols, and L Alvarez. Phonons in single wall carbon nanotube bundles. *Carbon*, 40(10):1697–1714, August 2002. doi:10.1016/s0008-6223(02)00010-6.

[34] Wenbo Wang, Hanna McGregor, Michael Short, and Haishan Zeng. Clinical utility of raman spectroscopy: current applications and ongoing developments. *Advanced Health Care Technologies*, page 13, June 2016. doi:10.2147/ahct.s96486.

[35] Ken-ichi Sasaki. Basic principles of raman spectroscopy for graphene. *NTT Technical Review*, 11(8):10–14, August 2013. doi:10.53829/ntr201308fa2.

[36] S. Costa, Ewa Borowiak-Palen, Marta Kruszynska, A. Bachmatiuk, and Ryszard Kalenczuk. Characterization of carbon nanotubes by raman spectroscopy. *Materials Science- Poland*, 26, January 2008. URL: https://www.materialsscience.pwr.edu.pl/bi/vol26no2/articles/ms_2007_54INMAT23.pdf.

[37] J.B. Bates. Fourier transform infrared spectroscopy: The basic principles and current applications of a rapidly expanding technique are reviewed. *Science*, 191(4222):31–37, January 1976. doi:10.1126/science.1246596.

[38] Aljoscha Roch, Lukas Stepien, Teja Roch, Ines Dani, Christoph Leyens, Oliver Jost, and Andreas Leson. Optical absorption spectroscopy and properties of single walled carbon nanotubes at high temperature. *Synthetic Metals*, 197:182–187, November 2014. doi:10.1016/j.synthmet.2014.09.016.

[39] Stéphane Berciaud, Laurent Cognet, Philippe Poulin, R. Bruce Weisman, and Brahim Lounis. Absorption spectroscopy of individual single-walled carbon nanotubes. *Nano Letters*, 7(5):1203–1207, March 2007. doi:10.1021/nl062933k.

[40] Sergei M. Bachilo, Michael S. Strano, Carter Kittrell, Robert H. Hauge, Richard E. Smalley, and R. Bruce Weisman. Structure-assigned optical spectra of single-walled carbon nanotubes. *Science*, 298(5602):2361–2366, December 2002. doi:10.1126/science.1078727.

[41] R. Bruce Weisman and Sergei M. Bachilo. Dependence of optical transition energies on structure for single-walled carbon nanotubes in aqueous suspension: An empirical kataura plot. *Nano Letters*, 3(9):1235–1238, August 2003. URL: http://dx.doi.org/10.1021/nl034428i, doi:10.1021/nl034428i.

[42] Y. Oyama, R. Saito, K. Sato, J. Jiang, Ge. G. Samsonidze, A. Grüneis, Y. Miyauchi, S. Maruyama, A. Jorio, G. Dresselhaus, and M.S. Dresselhaus. Photoluminescence intensity of single-wall carbon nanotubes. *Carbon*, 44(5):873–879, April 2006. doi:10.1016/j.carbon.2005.10.024.

[43] K. Enge, E. Elmquist, V. Caiola, N. Rönnberg, A. Rind, M. Iber, S. Lenzi, F. Lan, R. Höldrich, and W. Aigner. Open your ears and take a look: A state-of-the-art report on the integration of sonification and visualization. *Computer Graphics Forum*, 43(3), June 2024. doi:10.1111/cgf.15114.

[44] Glenn F. Knoll. *Radiation Detection and Measurement*. John Wiley and Sons (WIE), Brisbane, QLD, Australia, 4 edition, August 2010.

[45] Slivia Dini, Luca Andrea Ludovico, Sergio Mascetti, and Maria Joaquina Valero Gisbert. Translating color: Sonification as a method of sensory substitution within the museum. In *20th International Web for All Conference*, W4A '23, page 162–163. ACM, April 2023. doi:10.1145/3587281.3587706.

[46] Sofia Cavaco, J. Tomás Henriques, Michele Mengucci, Nuno Correia, and Francisco Medeiros. Color sonification for the visually impaired. *Procedia Technology*, 9:1048–1057, 2013. doi:10.1016/j.protcy.2013.12.117.

[47] Walker Smith. Interactive musical periodic table: Sonification of visible element emission spectra. *"SMC paper"*, 2024. URL: https://smcnetwork.org/smc2024/papers/SMC2024_paper_id192.pdf.

[48] Florbela Pereira, João C. Ponte-e Sousa, Rui P. S. Fartaria, Vasco D. B. Bonifácio, Paulina Mata, Joao Aires-de Sousa, and Ana M. Lobo. Sonified infrared spectra and their interpretation by blind and visually impaired students. *Journal of Chemical Education*, 90(8):1028–1031, July 2013. doi:10.1021/ed4000124.

[49] Neil Garrido, Anaïs Pitto-Barry, Joan J. Soldevila-Barreda, Alexandru Lupan, Louise Comerford Boyes, William H. C. Martin, and Nicolas P. E. Barry. The sound of chemistry: Translating infrared wavenumbers into musical notes. *Journal of Chemical Education*, 97(3):703–709, February 2020. doi:10.1021/acs.jchemed.9b00775.

[50] Thierry Delatour. Molecular music: The acoustic conversion of molecular vibrational spectra. *Computer Music Journal*, 24(3):48–68, September 2000. doi:10.1162/014892600559335.

[51] M. Pietrucha. Sonification of spectroscopy data. Master's thesis, Worcester Polytechnic Institute, 2019. doi:CorpusID:210707140.

[52] Micaela M. Thiery. *Advanced Uses for Carbon Nanotubes: A Spherical Sound Source and Hot-films as Microphones*. PhD thesis, Michigan Technological University. doi:10.37099/mtu.dc.etdr/385.

[53] Lin Xiao, Zhuo Chen, Chen Feng, Liang Liu, Zai-Qiao Bai, Yang Wang, Li Qian, Yuying Zhang, Qunqing Li, Kaili Jiang, and Shoushan Fan. Flexible, stretchable, transparent carbon nanotube thin film loudspeakers. *Nano Letters*, 8(12):4539–4545, October 2008. doi:10.1021/nl802750z.

[54] Martin Russ. *Sound Synthesis and Sampling*. Routledge, November 2012. doi:10.4324/9780080481043.

[55] Scott Wilson, David Cottle, and Nick Collins. *The SuperCollider Book*. The MIT Press, 2011. doi:10.5555/2016692.

[56] Markus Leitgeb. *Photoelectrochemical Porosification of Silicon Carbide for MEMS*. PhD thesis, August 2020. doi:10.13140/RG.2.2.17410.09923.

[57] Niklas Rönnberg. Procedural sound design for user interfaces, 2025. [Accessed 05-05-2025]. URL: `lisam.liu.se`.

[58] Edgar Berdahl and Julius O. Smith III. Harmonic content of a plucked string -part 1: Single note, 2008. [Accessed 02-04-2025]. URL: `https://ccrma.stanford.edu/realsimple/harmonics/Part_1_Single_Note.html`.

[59] Meera Blattner, Denise Sumikawa, and Robert Greenberg. Earcons and icons: Their structure and common design principles. *Human-Computer Interaction*, 4(1):11–44, March 1989. `doi:10.1207/s15327051hci0401_1`.

[60] Nik Sawe, Chris Chafe, and Jeffrey Treviño. Using data sonification to overcome science literacy, numeracy, and visualization barriers in science communication. *Frontiers in Communication*, 5, July 2020. `doi:10.3389/fcomm.2020.00046`.